How do regulated thin filaments with hypertrophic cardiomyopathy-linked α-cardiac actin affect actomyosin interactions?

by

Haidun Liu

A Thesis
Presented to
The University of Guelph

In partial fulfillment of requirements
for the degree of
Master of Science
in
Molecular and Cellular Biology

Guelph, Ontario, Canada

Abstract

How do regulated thin filaments with hypertrophic cardiomyopathy-linked α-cardiac actin affect actomyosin interactions?

Haidun Liu
University of Guelph, 2017

Advisor:
Dr. John F. Dawson

Hypertrophic cardiomyopathy (HCM) is a heart disease associated with substitution mutations of sarcomeric proteins. This thesis describes investigations of the effects of mutations in α-cardiac actin (ACTC) subdomain 1 (E99K, R95C, F90Δ, and H88Y) on actomyosin interactions. ACTC proteins were expressed in a *Sf*21/baculovirus system and used in biochemical and biophysical assays to calculate the duty ratio (*r*). Compared to human ACTC (WTrec), E99K, R95C, F90Δ, and H88Y yielded higher, lower, or similar *r*. The varying *r* suggested that actomyosin changes may occur at the level of regulation by troponin and tropomyosin. Compared to WTrec regulated thin filaments (RTFs), R95C RTFs yielded no changes in *r* and E99K RTF yielded a decreased *r*, suggesting that the binding of myosin to actin may not be altered. However, E99K and R95C RTFs showed lower sensitivity to calcium, suggesting the altered cross-bridge cycling rate might lead to HCM.

Acknowledgements

I would like to thank Dr. John Dawson for taking me on as a graduate student in his laboratory and giving me the opportunity to contribute to cardiovascular disease research. He was an excellent advisor to me by offering his expertise, challenging me to think critically, and creating a fun and exciting environment. I would also like to thank Dr. Tami Martino and Dr. Todd Gillis for being part of my advisory committee members and offering their guidance and perspective during my studies. I greatly appreciate the time and counsel that they were able to give me whenever I needed help. For helping me survive doing microscope work for IVM assay, I want to thank Dr. Michaela Studer-Kype.

I thank the Heart and Stroke Foundation of Canada for providing the funding for our cardiovascular research and to host yearly Ride for Heart event in Toronto!

To the past and present members of Dawson Lab: Maria Anillo, Vadika Mishra, Mati Ojehemon, Michael Brodzikowski, Jessica Wong, Navneet Sidhu, Mary Henein, Grace Tseng, Tim Nguyen, Evan Despond, Zeeshan Shaikh, Klara and Kailey Beeney, Bernice Lau, and Love Sandhu- thank you for your contributions; you guys are the best.

Honorable mentions to Amanda Poole, Sherise Charles, Jozsef Varga, Piriththiv Dhavarasa, and residents of second floor, thank you all for being part of my journey here at Guelph.

Also, to my friends, family, and Doris Wong who supported through the harshest times to celebrating great moments, I definitely could not have done any of it without you.

Finally, all of this is made possible by and through our Heavenly Father, who has blessed me so much with friends and family. Everything that I learned and studied at Guelph has pointed to our Creator in Heaven and it has continuously to be mind-blowing. May He be glorified, forever and ever!

Table of Contents

List of Figures

List of Tables

List of Abbreviations

Actomyosin	Actin and myosin interaction
ABP	Actin binding protein
ACTC	α-cardiac actin gene
AcMNPV	*Autographa californica* multiple nucleopolyhedrovirus
BSA	Bovine serum albumin
CVD	Cardiovascular disease
DCM	Dilated cardiomyopathy
DEAE	Diethylaminoethyl cellulose
F-actin	Filamentous actin
FAST	Fast Automated Spud Trekker Manual
HCM	Hypertrophic cardiomyopathy
h.p.i.	Hours post-infection
IVM	*In-vitro* motility assay
MyBP-C	Myosin binding protein C
MOI	Multiplicity of infection
β-MHC	β-myosin heavy chain
Ni-NTA	Nickel- nitrilotriacetic acid
OD	Optical density
pCa	Logarithmic measure of calcium ion concentration

pCa_{50}	pCa at half of maximal activity
PIBs	Polyhedral inclusion bodies
RTF	Regulated thin filament
*Sf*21	*Spodoptera fugiperda* cell line clone 21
cTM	Cardiac tropomyosin
TM	Tropomyosin
cTnC	Cardiac troponin C
cTnI	Cardiac troponin I
cTnT	Cardiac troponin T
cTn	Cardiac troponin complex
Tn	Troponin
WTrec	Recombinant *wild type* ACTC

Chapter 1 – Introduction

1.1 Cardiovascular Disease

Cardiovascular diseases (CVDs), including disorders of the heart and blood vessels, are among the leading cause of death worldwide (World Health Organization, 2016). According to the World Health Organization, an estimated 17.5 million people died from CVDs worldwide in 2012; it is speculated that by 2030, this number will increase to more than 23 million each year (World Health Organization, 2016). Due to the negative effects of globalization, rapid unplanned urbanization, and increasingly sedentary lifestyles, it is reported that over 80% of CVDs take place in low- and middle-income countries (WHO, 2010). With the expected rise in mortality from heart diseases, many countries will have difficulties in finding the resources for policies, legislation, services, and infrastructure regarding CVD (Bloom et al., 2011). The impact of this increased strain to healthcare systems, individuals, families, businesses, and governments was estimated to cost the world's most populous nations $863 billion in 2010 and estimated to rise to $1044 billion by 2030 (Bloom et al., 2011). Thus, research on CVD is important to understand the underlying causes and to develop treatments to combat the rising mortality and economic burden caused by these diseases.

1.2 Hypertrophic Cardiomyopathy (HCM)

A subset of CVDs are cardiomyopathies, diseases attributed to the heart muscle. Although many symptoms and treatments have been found, there is still much about

cardiomyopathies that remains unknown. These diseases may develop from genetic or environmental factors such as diet and exercise (Chung et al., 2003) and can be further categorized into dilated cardiomyopathy (DCM) or hypertrophic cardiomyopathy (HCM). HCM is the focus of this thesis and is characterized by an asymmetrical change of the heart having a thickened left ventricular wall, enlargement of cardiomyocytes, and overall stiffness of the heart (Wigle et al., 1985). Due to these morphological changes, the heart muscle must work harder by increasing the heart rate to compensate for the decreased volume of blood being pumped by the left ventricle to the rest of the body (American Heart Association, 2016). If the heart muscle cannot pump sufficient blood out to the rest of the body, then symptoms such as chest pain, dizziness, shortness of breath, fainting, and worst of all, heart failure can occur (American Heart Association, 2014). Hence, temporary medication such as β-blockers and calcium channel blockers are used to slow the heart rate, reduce myocardial oxygen demands, and increase the ventricular filling time by relaxing the muscle to bring the cardiac output back to normal (Daughenbaugh, 2007). With the elevated heart rate in patients with HCM after exercise (Patel et al., 2014), there must be changes at the sarcomeric level that leads to this disease state. Specifically, I will be looking at myocardial contractility: the ability of the heart to produce force resulting from actin and myosin interactions (Katz, 1967).

1.3 Sarcomere

The basic unit of contractility in the heart muscle is the sarcomere, which has a striated appearance from arrays of dark bands (myosin) and light bands (actin). The sarcomere is composed of different regions and components as seen in **Figure 1A**. The

major contractile proteins in the heart muscle are α-actin (*ACTC*) and β-myosin which interact to convert chemical energy into mechanical force. In the resting state, myosin and actin filaments overlap in the peripheral regions of the A band, while the middle region H zone has only myosin filaments. During muscle contraction, the myosin pulls the actin inwards to the M line, which causes shortening of the sarcomere (Cooper & Hausman, 2007). How ACTC and β-myosin interact, along with the key regulatory proteins cardiac-troponin (*cTn*) and cardiac-tropomyosin (*cTM*) will be discussed in sections **1.8 and 1.10**. The global hypothesis is that HCM is caused by impaired contractile performance of the sarcomere, leading to the compensatory hypertrophy of heart (Mogensen et al., 1999).

1.4 Genetics of HCM

HCM is associated with point mutations in genes encoding contractile proteins (Redwood et al., 1999; Seidman & Seidman, 2001). These mutations may exert their pathological effects by disrupting biological pathways and protein interactions (Song et al., 2011). The underlying molecular basis for differing phenotypes such as HCM and DCM is however unknown, and no clear mechanistic hypothesis exists (Moore et al., 2012; Song et al., 2011). Studying each amino acid residue difference of all the sarcomeric proteins and finding links to disease is not practical. Fortunately, studies of the heart in patients and animal models have identified a set of mutations that can alter protein functions, leading to cardiomyopathies (Moore et al., 2012; Morimoto, 2008).

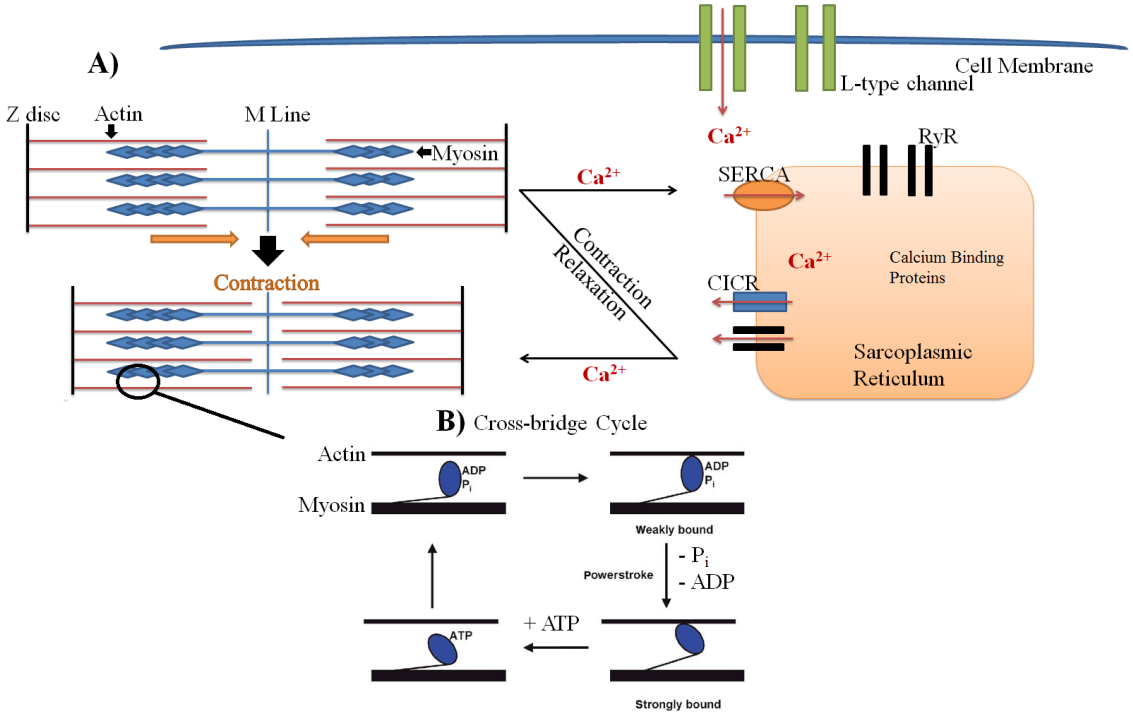

Figure 1. Schematic diagram of cross-brdige cycle and role of calcium in contraction. During contraction, actin "slides" on myosin to creates a broader width of overlaps between filaments. (**A**) Briefly, calcium enters myocytes through the L-type channels and enters the sarcoplasmic reticulum through complex cell signaling, via SERCA proteins or sequestered into the myoplasm through RyR and CICR membrane proteins. During contraction, calcium is sequestered into the myoplasm where it binds to sarcomere protein filaments and initiates actomyosin interactions. During relaxation, calcium is pumped back into the sarcoplasmic reticulum and also pumped out of the cell (not shown) through the Na^{+}-Ca^{2+} exchanger. (**B**) Starting from bottom right, myosin is tightly bound to actin in absence of ATP. When ATP is bound to the myosin head, it undergoes a conformational change and dissociates from actin. ATP is hydrolyzed in the enzymatic region of myosin and releases ADP and inorganic phosphate (Pi). Removal of products allows the myosin head to bind to the actin once again and perform a power stroke by pushing the actin towards the M line. Figure obtained with permission from Goody (2003).

Protein interactions are at the core of normal heart muscle function. Substitution mutations in genes encoding sarcomeric proteins can affect overall muscle contraction and result in either hypercontractility or hypocontractility defined as higher or lower force resulting from altered actomyosin cycling, respectively (Marian & Roberts, 2001; Redwood et al., 1999). Although changes in different sarcomeric proteins led to different changes in contractility, they can lead to the same disease state. The cause for different sarcomeric proteins leading to either hypercontractility or hypocontractility may due to the function of each sarcomeric protein. The three genes that account for three-fourths of all HCM cases are β-myosin heavy chain (β-MHC), myosin binding protein C (MyBP-C), and cardiac troponin T (cTnT). Of interest are the genes that encode sarcomeric proteins that are responsible for contraction.

The majority of biophysical and biochemical studies of amino acid residue changes in myosin result in decreased actin-activated ATPase assay, decreased filament velocity, and overall reduced force production (Redwood et al., 1999). Conversely, studies on mutations in the cTnT gene showed both increased calcium sensitivity, correlating with higher contractility, and decreased calcium sensitivity, correlating to lower contractility (Sweeney et al., 1998). Studies of substitution mutations of TM resulted in increased filament velocity and increased calcium sensitivity indicating hypercontractility (Karibe et al., 2001). My thesis will specifically look at mutations of one sarcomeric protein that has a major role in muscle contraction similar to myosin, but has not been well characterized in HCM: α- cardiac actin (*ACTC)*.

1.5 α-cardiac actin (*ACTC*) gene mutations

Missense mutations within the ACTC gene can manifest anywhere on the protein's four subdomains affecting either the internal properties of actin or its interactions with actin-binding proteins. These changes can lead to problems with force generation or force transmission. To date, there are 16 ACTC substitution mutations found in patients with cardiomyopathy, with 12 associated with HCM: E99K (Olson et al., 2000), P164A (Olson et al., 2000), Y166C (Mogensen et al., 2004), A230V (Van Driest et al., 2003), A295S (Mogensen et al., 1999) , M305L (Mogensen et al., 2004), S271F (Olivotto et al., 2008), A331P (Olson et al., 2000), H88Y (Morita et al., 2008), R95C (Morita et al., 2008) , F90Δ (Kaski et al., 2009) , and R312C (Kaski et al., 2009). Four substitution mutations are linked to DCM: E361G (Olson et al., 1998), R312H (Olson et al., 1998), T126I (Lakdawala et al., 2012), and I250M (Lakdawala et al., 2012) (**Figure 2A**). My work will focus on the known mutations in subdomain 1 of ACTC (E99K, R95C, F90Δ, and H88Y) that might cause molecular dysfunction in the actomyosin complex leading to HCM.

The ACTC E99K mutation was among the first mutation in the ACTC gene discovered in patients with cardiomyopathy (Olsen et al., 2000). The ACTC E99K mutation was found in 7 out of 319 patients from ages 25-67 that had left ventricular hypertrophy. This mutation was considered to be autosomal dominant due to individuals inheriting HCM from family members (Olson et al., 2000). The ACTC F90Δ mutation was a novel mutation found in <5% of 42 individuals that were diagnosed at age 13 or younger during their growth sprout (Kaski et al., 2009). In addition, these patients' first-degree relatives were also found to be affected by HCM, and the second-degree relatives

were classified as carriers of this mutation because they had normal heart echocardiograms (Kaski et al., 2009). Similarly, the ACTC R95C and H88Y mutations were found as part of a screen of 84 children diagnosed with cardiomyopathy before age 15 (Morita et al., 2008). These two mutations are presumed to be sporadic due to a lack of symptoms observed initially (Morita et al., 2008).

1.6 Actin

Actin was first isolated in 1942 by Bruno Ferenc Straub from muscle cells. It is roughly a 42 kDa protein containing four distinctive subdomains with a nucleotide binding site. Although actin was first thought to function only in muscles, it has been found in all cell types throughout the body. In mammalian cells, six isoforms of actin exist (**Figure 2B**); all isoforms have subtle sequence variation, yet possess different functions. The focus of this thesis is α-cardiac actin (*ACTC*), which is one of the core motor proteins responsible for heart contraction (Kumar et al., 1997; Vandekerckhove et al., 1986). One major property of actin is its ability to polymerize and form stable filamentous actin (F-actin) in the presence of salt compounds and ATP (Straub, 1942, 1943; Mommaerts 1950). Previous studies in our lab have shown that ACTC subdomain 1 variants F90Δ, H88Y, R95C, and E99K polymerize normally after purification with only subtle changes in nucleation and elongation phases (Anillo, 2015; Mundia et al., 2012). Since only subtle changes have been found in the intrinsic properties of these HCM associated ACTC subdomain 1 variants, the primary cause for HCM may not be the actin itself, but the interaction of actin and myosin.

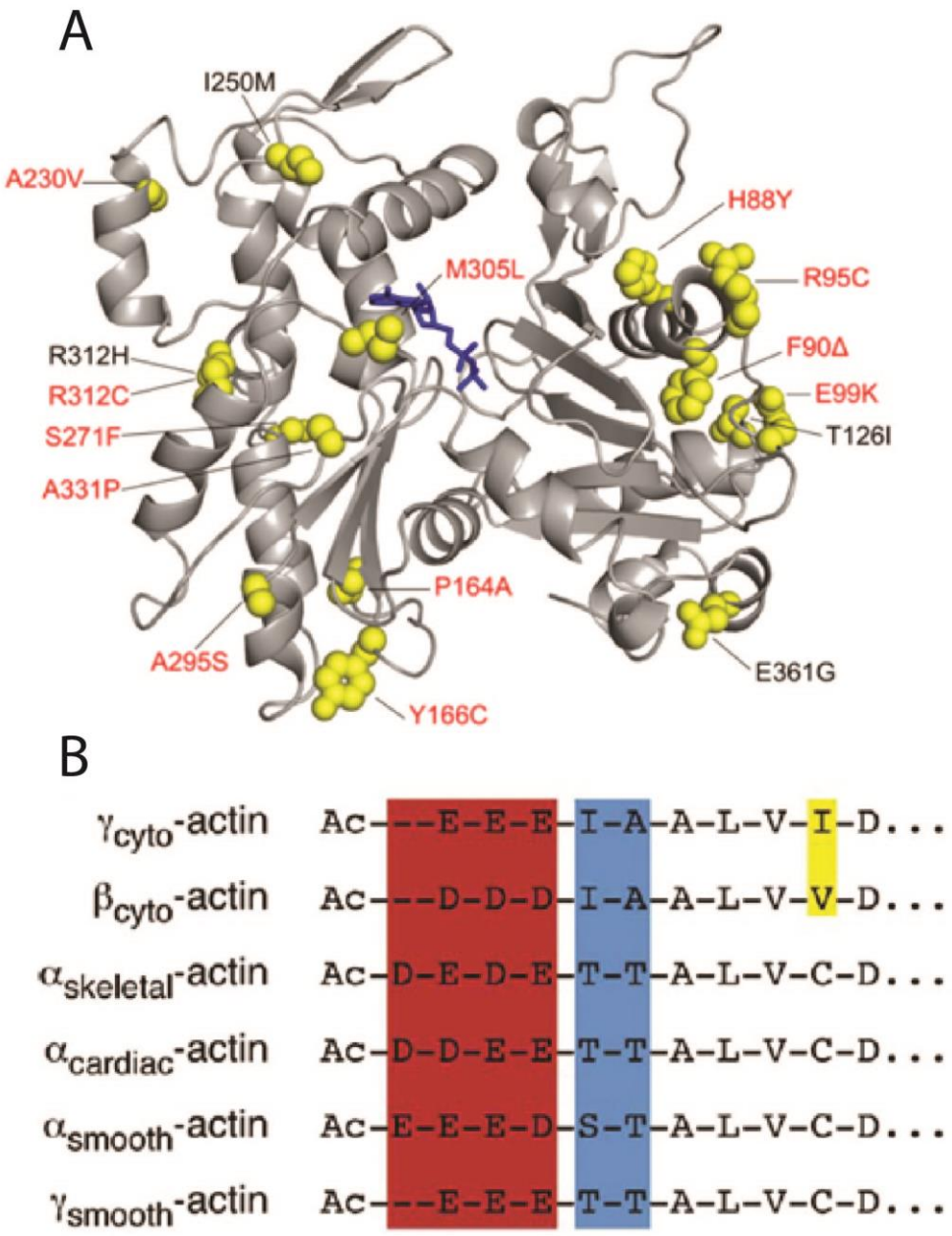

Figure 2. Actin and isoactins. (**A**) In the ribbon model, actin contains 4 subdomains with a nucleotide in the middle that holds the molecule in its native form: subdomain 1 (residues 1-32, 70-144, and 338-374), subdomain 2 (residues 33- 69), subdomain 3 (residues 145-180 and 270-337), and subdomain 4 (residues 181- 269). The substitution mutations indicated in red are associated with HCM, while those in black are associated with DCM. (**B**) N-terminal sequences of the 6 mammalian actin isoforms. Red residues exhibit the most variability within the isoactins. Blue residue differences occur primarily between cytoplasmic and muscle isoforms. Yellow residues vary between the β- and γ-cytoplasmic isoactins. Figure used with permission from Perrin & Ervasti (2010).

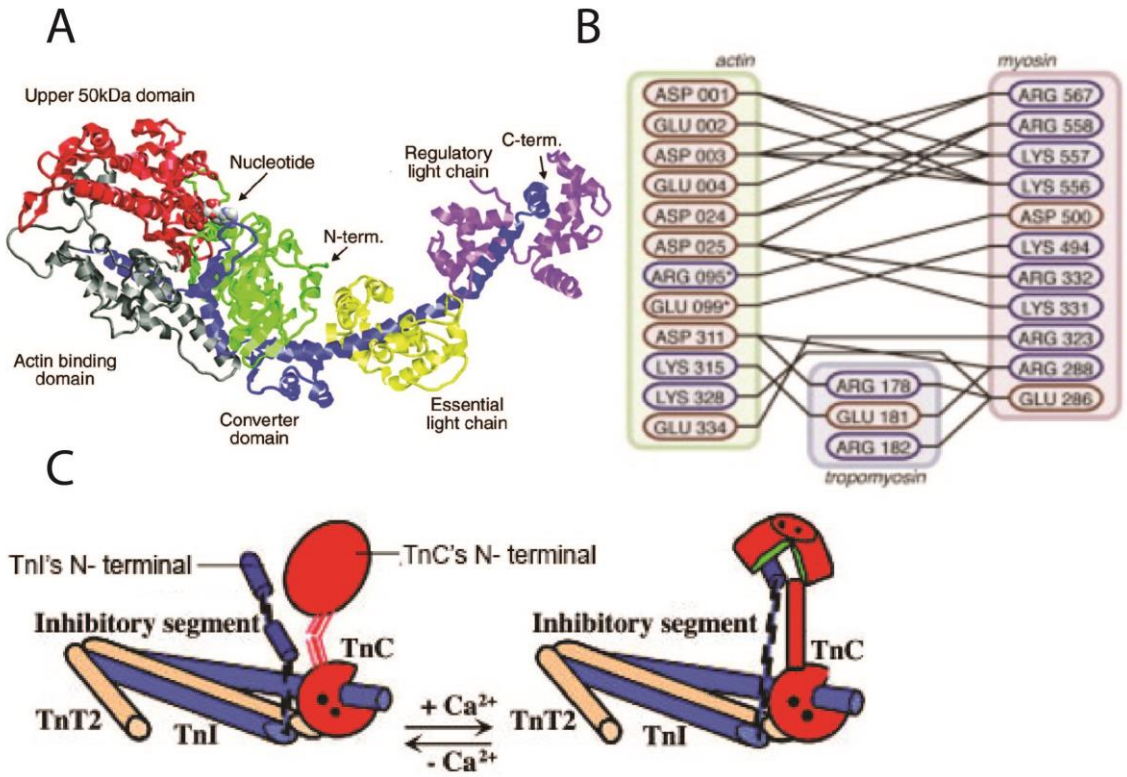

Figure 3. Schematic diagram of three ABPs and possible contacts with actin. (**A**) The myosin head and neck comprise the subdomain 1 fragment (S1) containing enzymatic ATPase activity and the location for actin binding. Figure obtained from Ruegg et al. (2002). (**B**) The possible electrostatic interactions between actin, tropomyosin, and myosin. Figure used with permission from Behrmann et al. (2012). (**C**) The troponin complex undergoes conformational change in response to calcium: TnI (blue), TnC (red), and TnT (beige). In the presence of calcium, TnC's N-terminal self-binds to TnI's N-terminal; it dissociates upon absence of calcium. Figure obtained from Vinogradova et al. (2005).

1.7 Myosin

As mentioned earlier, there is extensive research on myosin and its link to HCM. Jarcho et al. (1989) was the first group to find a mutation in the β-myosin heavy chain (*β-MHC*) gene that was linked to HCM. Myosin, like actin, is found in a wide variety of eukaryotic cells. There are at least 17 different classes of myosin based on their amino acid sequences. One major characteristic found in all types of myosin proteins is a motor head domain that contains an actin binding site and hydrolyzes ATP to drive the myosin motor in contractile fibres (**Figure 3A**). In the heart, two MHC isoforms exist: α- and β-MHC. My thesis will use β-MHC in biophysical and biochemical assays due to it being upregulated in failing hearts (Carniel et al., 2005).

1.8 Actomyosin Complex

Cardiac muscle is powered by ATP-dependent interactions of actin and myosin (Moore et al., 2012). As shown in **Figure 1B**, myosin undergoes ATP hydrolysis that affects its conformation, and the binding of actin (Seidman & Seidman, 2001). These changes form the basis of cross-bridge cycling and the process of contraction.
An analogy to understand this actomyosin complex is a train on a track. Long F-actin represents the track of a railroad, while myosin is the locomotive that produces the pulling power to move the train. Just as a steam train is fueled by burning combustible material to move along the track, myosin uses ATP to move along actin.

Studies have revealed that the contacts between actin and myosin involve several residues located in myosin loops and the residues in subdomains 1 and 3 of one actin subunit (Behrmann, 2012; Bookwalter & Trybus, 2006). Specifically, R95 and Y91 in

actin subdomain 1 form hydrogen bonds with residues in loop 3 of myosin (Lorenz & Holmes, 2010). Electrostatic interactions are also thought to exist between residues on subdomain 1 of actin (R95 and E99) and myosin S1 (D500 and K494) (**Figure 3B**) (Behrmann, 2012). If these key amino acid residues are altered, the electrostatic forces between actin and myosin filaments may be changed and affect the overall contractile force produced by sarcomere (Behrmann, 2012).

1.9 Duty Ratio

The ensemble force is the force produced by the interaction between myosin heads and actin; it can also be described by the formula: $F_{En} = f \cdot r \cdot N_T$, where f is the force produced by each myosin head, r is the duty ratio of myosin, and N_T is the total number of myosin heads forming interactions with actin (Sommese et al., 2013). Hence, an increase or a decrease in any one of the variables will lead to a higher or lower ensemble force within the sarcomere, correlating to either hypercontractility or hypocontractility and contributing to the development of HCM (Sommese et al., 2013).

Of interest, the duty ratio is a biophysical characteristic of actomyosin interactions, defined as the proportion of the ATPase cycle with myosin bound to actin filaments (De La Cruz et al., 1999). The duty ratio can be calculated using the formula: $r = \delta \cdot k_{cat}/v_o$, where δ is the stepsize of myosin, k_{cat} is the turnover number of ATP hydrolysis by myosin, and v_o is the myosin motor velocity. Assuming a constant step size for myosin of 5 nm (Molloy et al., 1995), the duty ratio may be determined for the actomyosin interaction in the presence of filaments composed of recombinant human wild type ACTC (WTrec) or ACTC variant proteins expressed in an *Sf*21/baculovirus

system. Actin-activated ATPase assays can be used to determine the enzymatic activity and obtain k_{cat} values, while *in vitro* motility (IVM) assays provide information on cross-bridge cycles through obtaining individual filament's v_o values. The calculated duty ratio in the presence of ACTC variants may shed light on the effects that alterations in actin have on contraction.

Bookwalter and Trybus (2006) shown that interactions between substitution mutation of E99K in ACTC and myosin alone resulted in reduced affinity of myosin for actin and decreased force generation. Decreased force can be the result of decreased duty ratio, correlating to lower sarcomere ensemble force and hypocontractility, as myosin spends less of the cross-bridge cycle bound to actin and lowers ATPase activity (Harris & Warshaw, 1993). Due to the findings of various substitution mutations in myosin resulting in hypocontractility (Redwood et al., 1999) and that ACTC is a critical partner with myosin:

I hypothesize that HCM-linked ACTC variants R95C, H88Y, E99K, or F90Δ cause defects in contractility resulting from decreased duty ratios relative to WTrec ACTC.

1.10 Troponin/Tropomyosin (Tn/TM)

At the physiological level, sarcomere contraction does not occur with actin and myosin alone; therefore, other relevant proteins must be considered. My thesis will focus on the additional regulatory proteins Tn and TM that bind to actin and form regulated thin filaments (RTFs). Returning to the analogy of the locomotive on a track, Tn and TM represent a motor's governor, a device that measures and regulates the speed of an

engine. Similarly, Tn and TM bind to actin to regulate the enzymatic activity of actomyosin, modulated by the presence of calcium.

The interaction between actin and Tn-TM in a calcium-dependent manner can be described by the steric blocking model of thin filament regulation (Huxley, 1973; Parry & Squire, 1973). The model shows RTFs in two states. One state is the "off" position where in absence of calcium, TM physically blocks the actin from binding to actin. The second state is the "on" position where in presence of calcium, Tn moves the TM and expose the site on actin that binds to myosin. Furthermore, equilibrium and kinetic studies of RTFs by McKillop and Geeves (1993) suggests a three-state model that includes the "open" state that is the same as the "on" position, but the "off" state is broken down into two states: a "closed" state where myosin weakly binds in the presence of an intermediate amount of calcium and partially reveals the actin sites, and a "blocked" state that is analogous to the "off" state.

In RTFs, TM is bound to actin and inhibits the myosin binding site on actin (Huxley, 1973). There are three isoforms of TM that are expressed to varying degrees depending on the species and age of animals (Scellini et al., 2014; Shchepkin, Kopylova, & Nikitina, 2011). My work will utilize α-tropomyosin1 (α-TM1) which is primarily expressed primarily in human hearts (Shchepkin et al., 2011). Referring to **Figure 3B**, subdomain 3 residues of actin play a significant role in interaction with TM and myosin. D311 from actin subdomain 3 is thought to form electrostatic interactions with R178 on TM and R288 in a myosin loop. In addition, K315 of actin subdomain 3 forms electrostatic interactions with E181 of TM (Behrmann, 2012). Such interactions, if

altered, may also change the binding between regulated actin and myosin filaments, and affect the duty ratio of myosin and overall force produced by the sarcomere.

The other major regulatory protein, Tn, plays a major role in manipulating TM by undergoing a calcium-dependent conformation change. As depicted in **Figure 3C**, Tn is a complex of three non-identical subunits: troponin I (TnI), troponin T (TnT), and troponin C (TnC). Each subunit has a specific role during contraction and undergoes conformational changes depending on the presence of calcium. Similar to TM, there are various isoforms of each component of Tn depending on the age and type of muscle (Buzan, Du, Karpova, & Frieden, 1999; Farah & Reinach, 1995; Gomes, Potter, & Szczesna-cordary, 2002; Marion L Greaser & Gergely, 1973; Zot & Potter, 1987). In addition to TM, my thesis will utilize cardiac TnT, TnI, and TnC (cTnT, cTnI, and cTnC, respectively) in forming regulated thin filaments (RTFs).

1.11 Calcium handling

Calcium is stringently managed by many mechanisms in muscle such as the sarcoplasmic reticulum (SR), an organelle that stores calcium, and L-type calcium channels located in membranes of cardiomyocytes (**Figure 1A)** (Cooper & Hausman, 2007; Mackrill, 1999). Briefly, calcium is released into the cytosol from approximately 10^{-7} to 10^{-5} moles/liter (0.1-10 μM), resulting in muscle contraction via the action of Tn and TM as mentioned above in the steric hindrance model of RTFs (Cooper & Hausman, 2007). The movement of calcium within the cell is highly regulated by many membrane proteins, such as voltage-dependent L-type calcium channels and ATPase pumps (Gehlert et al., 2015; Marks, 2013; Ottolia, Torres et al., 2013; Zarain-Herzberg et al., 2012).

Sigmoidal relationships between calcium and muscle biophysical properties have been observed since late 1960s to mid-1970s (Best et al., 1977; Hellam & Podolsky, 1969; Donaldson & Kerrick, 1975; Fabiato & Fabiato, 1975; Weber & Murray, 1973). This relation can be described by the Hill's equation (1910) that was used to describe the cooperative binding of oxygen by hemoglobin. The origin of EC_{50} or pCa_{50} comes from substituting a constant from the Hill's equation. EC_{50} and pCa_{50} are defined as the amount of calcium required for half of maximal activity, and are useful for summarizing calcium sensitivity of muscles. Thus, a decrease in calcium sensitivity requires more calcium ions and an increase in calcium sensitivity requires less calcium ions to achieve midpoint muscle parameters such as myosin ATPase activity. The difference between pCa_{50} and EC_{50} values is having normal and log-normal distributions, respectively. Thus, Walker et al. (2010) recommend performing a log transformation before using statistical tests for EC_{50}. Furthermore, pCa_{50} or EC_{50} are useful variables for identifying calcium sensitivity. In this thesis, an EC_{50} equation was used to fit the activity-pCa and motility-pCa curves, and the term pCa_{50} is used instead of EC_{50} to clarify that varying concentrations of calcium ions are being tested.

The calcium sensitivity of the Tn-TM complex controls successful actomyosin cross-bridge formations in a normal functioning heart. To reiterate, changes in calcium sensitivity can be experimentally described as the pCa_{50} obtained from the relationship between force/motility and calcium concentration. Specifically, a decrease in calcium sensitivity (lower pCa_{50}) translates to less actomyosin interactions due to Tn-TM blocking the myosin-binding site on actin at normal calcium levels, resulting in

hypocontractility (MacIntosh, 2003). In continuation with the hypothesis that substitution mutations in ACTC subdomain 1 result in lower contractility:

I hypothesize that regulated actomyosin complexes including subdomain 1 ACTC variants linked to HCM will decrease the myosin duty ratios and calcium sensitivities correlating to lower contractility.

1.12 Research Aims

Multiple studies have linked genetic mutations in sarcomeric proteins to HCM as summarized by Seidman and Seidman (2001). 16 mutations in the *ACTC* gene encoding α-cardiac actin have been linked to cardiomyopathies, 12 of which develop into HCM. Of particular interest are the mutations located in subdomain 1 of actin (H88Y, F90Δ, R95C, and E99K) at the proposed actomyosin interface. Biophysical assays were used to test the interactions between ACTC variants and myosin, and the inclusion of regulatory proteins Tn and TM.

Aim 1: Purify ACTC variant proteins and myosin and determine their resulting duty ratios to test the hypothesis that HCM linked ACTC variants cause a decrease in contractility.

A. The turnover number of ATP hydrolysis by myosin, k_{cat} was determined from the V_{max} of Michaelis-Menten curves of myosin ATPase activity assay in the presence of HCM-linked ACTC variants.
B. Using an *in vitro* motility assay, I measured the myosin motor velocity, v_o, through the interaction of fluorescently labeled ACTC variants on a myosin bed.

Aim 2: Produce RTFs with purified regulatory proteins cTn and cTM to test the second hypothesis that HCM-associated RTF variants will exhibit lower duty ratio and calcium sensitivity.

A. I performed ATPase assay with RTF variants and myosin at varying pCa to determine the pCa_{50} of each ACTC variant.
B. I also used the *in vitro* motility assays to determine the filament velocities and movement of fluorescently labeled RTF variants at varying pCa to produce pCa curves as a function of RTF movement and velocity.

1.13 Summary and Importance

The myosin duty ratios varied with unregulated ACTC variants, contradicting my first hypothesis that the duty ratios for all subdomain 1 ACTC variant proteins would be lower than WTrec. In comparison to WTrec ACTC, E99K yielded an increased myosin duty ratio, H88Y yielded a similar myosin duty ratio, and F90Δ and R95C both yielded a decreased myosin duty ratio. Surprisingly, in the investigation with regulated ACTC variants and comparing the duty ratio values to WTrec, RTFs with R95C ACTC yielded a similar duty ratio and RTFs with E99K ACTC yielded a decreased duty ratio. In the ATPase rate-pCa curve profiles generated from myosin ATPase and motility/velocity-pCa curve profiles from IVM assays, RTFs with R95C and E99K ACTC had a higher pCa_{50} than WTrec RTF, indicating lower sensitivity to calcium. My results demonstrate different molecular dysfunctions may exist in HCM patients depending on the mutation, suggesting that different treatments targeting the specific dysfunction in sarcomeric proteins might be needed to alleviate the onset of the disease in individual cases.

Chapter 2 – Materials and Methods

2.1 Reagents

HiTrap DEAE fast flow columns (GE Healthcare, Piscataway, NJ) and Ni-NTA Superflow columns (Qiagen, Valencia, CA) were used for ACTC purification. SDS-PAGE gels were made using a 29:1 bisacrylamide solution obtained from Bio-Rad (Hercules, CA). Supplemented Grace's Insect Medium (1X), Fetal Bovine Serum (FBS), and Penicillin/Streptomycin (PenStrep) mix were obtained from Gibco (Life Technologies, Mississauga, ON).

2.2 Basic protocols

2.2.1 Protein concentration quantification

The concentrations of the purified α-cardiac actin tissue and ACTC protein variants were determined using actin standards of known concentration with a Bio-Rad Protein Assay dye reagent (Hercules, CA) and protocol outlined by the manufacturer. The protein concentrations were read at an absorbance at 595 nm. The concentrations of troponin and tropomyosin were determined by absorbance at 280 nm using a Beckman-Coulter DU800 Spectrophotometer with an extinction coefficient of $E^{1\%}$ 0.37 and 0.33, respectively (Gafurov & Chalovich, 2007). The concentration of myosin from rabbit *soleus* muscle was also determined by using absorbance at 280 nm using a Beckman-Coulter DU800 Spectrophotometer with an extinction coefficient of $E^{1\%}$ 5.3 (Margossian & Lowey, 1982).

2.2.2 Polyacrylamide gel electrophoresis

SDS-PAGE gels were made with a 10% polyacrylamide resolving gel and a 5% polyacrylamide stacking gel. All protein samples were mixed in a 1:2 ratio with 2x Laemmli buffer (50 mM Tris, pH 6.8, 2% SDS, 10% glycerol, 1.3 M βME and 0.1% bromophenol blue (Fisher Scientific, Whitby, ON)) (Laemmli, 1970) and loaded into the gels. The gels were run using 1x running buffer (25 mM Tris, 250 mM glycine, and 0.1% SDS (Fisher Scientific, Whitby, ON)) at 180 V for 40 min. The gels were then stained with Coomassie brilliant blue dye R-250 (Sigma Aldrich, Oakville, ON) for 40 min and destained for 40 min with destaining buffer (40% methanol and 10% acetic acid).

2.2.3 Cell culture

T25 monolayer flasks (Corning, NY) were used to maintain *Spodoptera frugiperda* (*Sf*21) insect cells. The cells were kept in a 27°C incubator and passaged every 3 days using supplemented 1x Grace's Insect Medium with 10% FBS and 1% PenStrep. Suspension cultures in 1 L Wheaton spinner flasks (Millville, NJ) were used to maintain larger cell densities meant for large-scale protein expression. A hemocytometer was used to count cells as described by Mather et al., 1998. The viability of the cells was monitored using a trypan blue stain (Fisher Scientific, Whitby, ON).

2.2.4 Western Blotting and Dot Blot

T25 monolayer flasks were seeded with *Sf*21 cells at a cell density of ~ $1x10^6$ cells/mL and infected with the titered ACTC recombinant virus at a multiplicity of infection (MOI) of 1. The infected cells were kept in a 27°C incubator and harvested after

72 h post infection (h.p.i.) via centrifugation at 4000 rpm for 10 min using an Eppendorf Centrifuge 5416 (Sigma-Aldrich, Oakville, ON). The harvested cell pellet was lysed using 1% NP-40 lysis buffer (1% NP-40, 150 mM NaCl, and 50mM Tris, pH 8.0 (Fisher Scientific, Whitby, ON)) for 10 min. The cell lysate was then mixed in a 1:1 ratio with 2x Laemmli buffer and run on a 10% SDS-PAGE gel. The protein in the gel was transferred onto a PVDF membrane (Sigma Aldrich, Oakville, ON) at 200 mA for 1 h at 4°C. The membrane was blocked using 5% skim milk powder dissolved in TBST (1x Tris-buffer saline, pH 7.4 with 0.1% Tween-20 (Fisher Scientific, Whitby, ON)) for 1 h at room temperature. The membrane was incubated in a 1:1000 dilution of an α-actin (5C5) mouse monoclonal primary antibody (Santa Cruz Biotechnology, Dallas, TX) and shook on a shaker (Barnstead Lab-line, Iowa, USA) set to 50 RPM overnight at 4°C. The membrane was washed 3 times for 5 min each with 1x TBST and probed with a 1:8000 dilution of a donkey anti-mouse secondary antibody (Applied Biological Materials Inc., Richmond, BC) for 50 min at room temperature. The membrane was washed 5 times for 5 min each with 1 x TBST and detected using ECL™ Western Blotting Detection reagents (Amersham, GE Healthcare, Piscataway, NJ). The film processor used to develop the film image was Konika Minolta SRX-101A (Konika Minolta Medical Imaging USA, Inc., Wayne, NJ).

A dot blotting protocol was similar to the Western blotting protocol. 5 uL of cell lysate samples were pipetted onto a nitrocellulose membrane (BioRad, Germany) and air dried. As with Western blotting, the membrane was blocked and incubated with primary antibody overnight before washing, probing with a secondary antibody, and visualizing.

2.3 Production of ACTC recombinant baculoviruses

2.3.1 Molecular cloning of α-cardiac actin protein variants

Mutagenex (Piscataway, NJ) performed site-directed mutagenesis on the pAcUW2Bmod-ACTC (WTrec) transfer vector to create the *ACTC* mutants (R95C, F90Δ, H88Y, and E99K). Verification of sequences for the pAcUW2Bmod-ACTC (mutants) was provided by the same company and also verified by Laboratory Services at University of Guelph.

2.3.2. Generation of ACTC recombinant baculoviruses

The generation of ACTC from *Sf*21/Baculovirus System protocol of Rutkevich et al. (2006) was followed (**Figure 4**). The pACUW2Bmod transfer vector containing the R95C, F90Δ, H88Y, E99K, mutant or WTrec inserts were co-transfected with *Bsu*36 I linearized BacPAK6 baculovirus DNA into *Sf*21 insect cells. This BacPAK system produces recombinant *Autographa californica* multiple nucleopolyhedrovirus (AcMNPV) expressing occlusion bodies / polyhedral inclusion bodies (PIBs). These PIBs are visible in the late infection phase of cells for visual recognition of viral infection and are used as a marker for viral amplification, titering, and viral infection cultures. After co-transfection, the concentration of recombinant virus may be very dilute such that PIBs are not readily observed. Thus, several amplifications of the virus through passaging of cell cultures may be required.

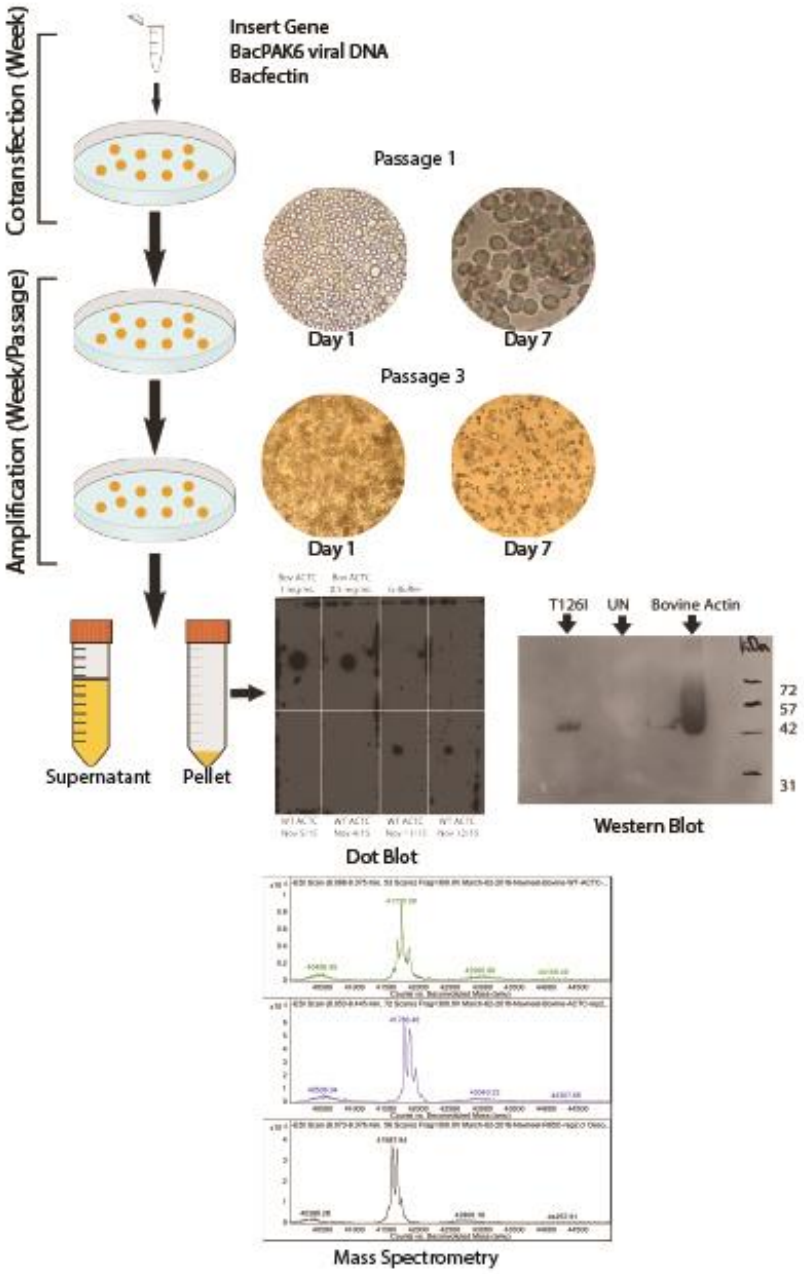

Figure 4. **Virus generation and confirmation of ACTC recombinants variants**. *Sf*21 Insect cell were co-transfected with baculovirus containing the ACTC mutant inserts. After 72 hours polyhedral inclusion bodies (PIBs) were not seen. However, after amplification of the virus through 3 passages, PIBs were visible. The amplified virus was then titred so that cell culture can be infected at a multiplicity of infection (MOI) of 1. Infected cells are then harvested and lysed to obtain the recombinant ACTC proteins. The identity of the protein is determined by mass spectrophotometer of purified proteins or Dot or Western Blotting with an anti-α-actin monoclonal antibody.

ACTC recombinant viruses were amplified by seeding T75 monolayer flasks (Life Technologies, Burlington, ON) with ~1 x 10^6 cells/ml with a total of 20 ml of Grace's insect supplemented media (Life Technologies, Burlington, ON). A total of 5 µl of ACTC recombinant virus was mixed evenly with the cells by gently rocking the flask The flask was kept in a 27°C incubator until cell lysis was evident for the majority of the cells in a Nikon TMS microscope field of view at 10x magnification (Nikon, Japan), which took 14 days. The amplified ACTC recombinant viruses were harvested via centrifugation at 4000 rpm for 10 min using an Eppendorf Centrifuge 5416 (Sigma-Aldrich, Oakville, ON) and the supernatant containing the viral particles was stored in a 50 ml conical tube (Corning, NY) at 4°C, and shielded from light using tin foil.

To determine the infectivity of the harvested ACTC recombinant viruses, the viruses were titered using end point dilution ($TCID_{50}$) methods outlined by O'Reilly *et al*., (1994). Ideally, titer values of at least 2 x 10^7-1 x 10^8 plaque forming units (pfu)/ml are acceptable to use for infections; therefore, three rounds of amplification were required to reach the ideal titer values.

To verify that the proteins obtained from infected cells cultures are the recombinant ACTC, proteins were purified as seen in the actin purification methods from large-scale infection and send to Mass Spectrophotometry Facility in the Advanced Analysis Centre at the University of Guelph to be analyzed. Further verification of recombinant ACTC from insect cells was accomplished through dot blot or Western blotting (see 2.2.4).

2.4 Purification of proteins

2.4.1 Purification of his-tagged G4-6

Gelsolin is an actin severing, capping and uncapping protein (Sun et al., 1999).The structure of gelsolin consists of six similar domains. The actin-severing activity is located in the N-terminal half while the C-terminal is responsible for calcium regulation and activation (Kolappan et al., 2003). Gelsolin domains 4-6 (G4-6) have a high affinity for actin (Kolappan et al., 2003). Due to the calcium regulation and its affinity for actin, G4-6 can be used to purify actin from many sources.

Overexpression of His-tagged G4-6 protein in E. *coli* cells is described by Ohki et al. (2009). E. coli cells are lysed using a French Press followed by centrifugation of 20,000 rpm for 30 minutes using Beckman-Coulter JA-20 rotor to obtain soluble G4-6 proteins. The mixture is then recirculated into a 5 mL Ni-NTA column (Qiagen, Montreal, QC) to allow the binding of His-tagged G4-6 to the Ni-NTA agarose. Buffer containing imidazole (Fisher Scientific, Whitby, ON) is used to replace and to elute the G4-6 from the column (**Figure 5A**). As seen in **Figure 5B**, there were still some contaminating proteins; thus, further purification was performed by size exclusion chromatography.

2.4.2. Purification of myosin protein from rabbit *soleus* muscle

The purification of myosin from rabbit *soleus* muscle was performed following the methods outlined by Margossian and Lowey (1982) using a freshly-killed New Zealand rabbit obtained from Abate Rabbit Packers (Arthur, ON). While at the abattoir, we ground the excised muscle and performed the first extraction by mixing the minced

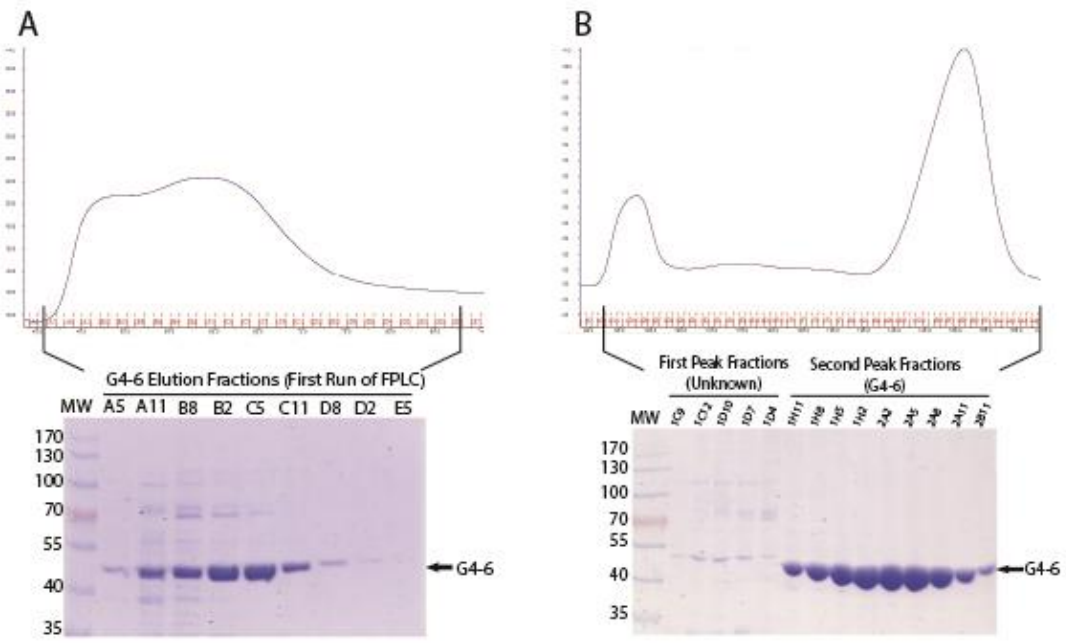

Figure 5. Purification of his-tagged G4-6. A. 10% SDS-PAGE showing purification of recombinant G4-6 from *E. coli* using a 5 mL Ni-NTA column. An imidazole gradient was used to elute the proteins. G4-6 (~45 kDa) appears in the fractions of the elution along with other contaminating proteins. B. 10% SDS-PAGE showing further purification of G4-6 using Sephacryl-300 gel filtration chromatography. As shown on the gel, high molecular weight and non-specific binding proteins were eluted in the first peak. Pure G4-6 was in the second peak.

meat with solution containing 0.3 M KCl, 0.15 M potassium phosphate, pH 6.5, 20 mM EDTA, 5 mM $MgCl_2$, and 1 mM ATP (Fisher Scientific, Whitby, ON). The extraction was stopped by diluting the mixture 4-fold with iced milliQ water and then kept on a bed of ice. Upon stopping the reaction, we immediately returned to Guelph which was ~40 min drive. The rest of the protocol was completed at the University of Guelph. Full-length myosin was stored in 50% glycerol and kept at -80°C. The myosin obtained from the soleus muscle of rabbits is a combination of >90% Type I (slow myosin; low ATPase activity) and <10% Type II (fast myosin; high ATPase activity) (Billeter et al., 1980; Reiser, Moss, Giulian, & Greaser, 1985). This is comparable to the myosin found in human cardiac ventricles which is a combination of <10% α-myosin heavy chain (high ATPase activity) and >90% β-myosin heavy chain (low ATPase activity) (Narolska et al., 2005; Reiser, Portman, Ning, & Schomisch Moravec, 2001).

2.4.2.1 Preparation of Heavy Meromyosin (HMM)

HMM was prepared following the protocol of Margossian and Lowey (1982) (**Figure 6**). Briefly, 0.2% α-chymotrypsin solution (2 mg/mL) (Sigma-Aldrich, Oakville, ON) was added to 2% myosin (20 mg/mL). The reaction occurs in room temperature for 10 min and was then stopped by adding PMSF (Fisher Scientific, Whitby, ON) to 0.3 mM. The solution was dialyzed overnight in 500 mL of solution containing 20 mM KCl, 10 mM potassium phosphate, pH 6.5, and 1 mM DTT to separate the soluble HMM from the insoluble LMM. The mixture was centrifuged at 50K RPM for 12 min and the supernatant collected. Protein concentrations in the supernatant were determined via

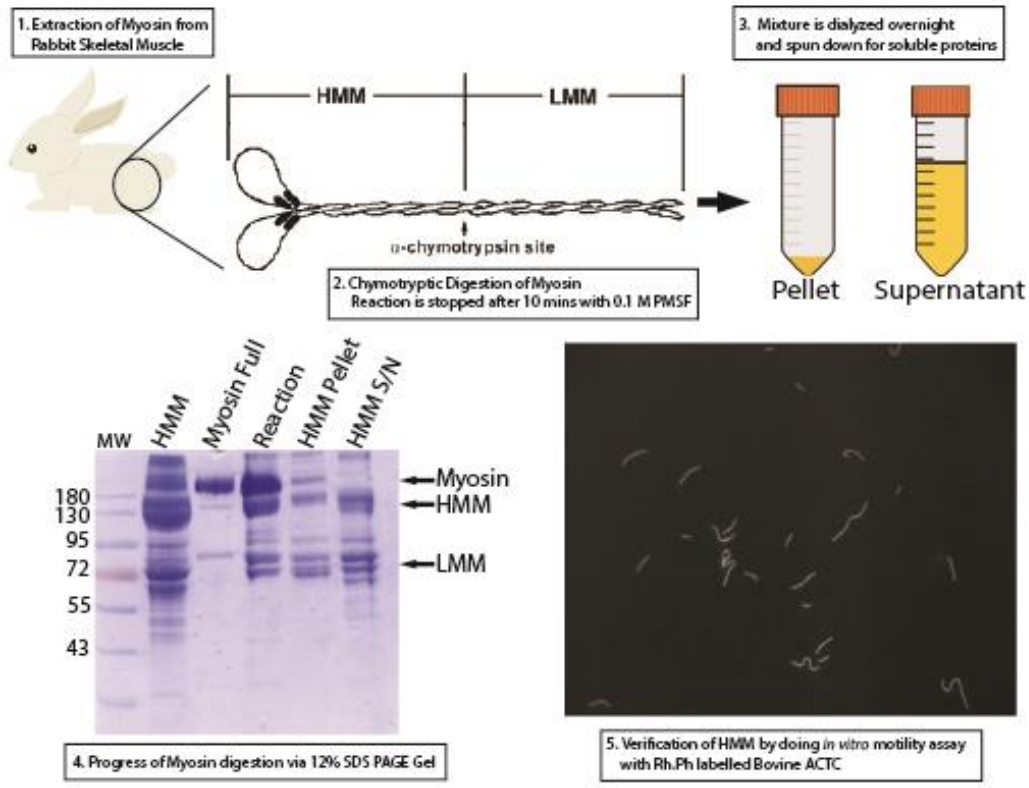

Figure 6. Purification of Heavy Meromyosin. Myosin was extracted from rabbit *soleus* muscle (1) as described by Margossian and Lowey (1999). Solution containing a-chymotrypsin was added to the myosin for 10 min to cleave the protein at the HMM/LMM junction (2). The reaction is then stopped by adding PMSF to 0.3 mM. The mixture is dialyzed overnight in low ionic conditions followed by centrifugation to separate the soluble HMM from the insoluble LMM (3). Samples were taken at each step of making HMM and run on a 10% SDS-PAGE gel stained with Coomassie to confirm the purity and presence of HMM and LMM (4). To confirm the activity of HMM, an in vitro motility assay was performed using the freshly cleaved HMM at concentrations of 0.125 mg/mL and rhodamine-phalloidin labeled actin filaments (5).

Bradford Assay (Bradford, 1976) and serial dilutions. Samples from each step were run on a 10% SDS-PAGE gel to confirm the presence of HMM.

2.4.3 Purification of bovine α-cardiac actin protein

α-cardiac actin protein was prepared from the left ventricular muscle of bovine hearts obtained from the Animal and Poultry Science Department (Guelph, ON) using the protocol outlined by Spudich and Watt (1971). Bovine α-cardiac actin was used as a control for all the assays performed as it shares 100% sequence identity to human α-cardiac actin protein (**Figure 7**).

2.4.4 Purification of ACTC variant proteins

We incorporated His-tagged G4-6 affinity and DEAE anion exchange chromatography in the purification of ACTC from *Sf*21 insect cells (**Figure 8**). Infected *Sf*21 insect cells were harvested by centrifugation at 4000 *g* for 15 min. Pellets were lysed with Buffer A (10 mM Tris, pH 8.0, 5 mM $CaCl_2$, 0.2 mM PMSF, 0.01 mg/mL Leupeptin, 1 mM ATP, 2 mM β-mercaptoethanol) and 2 g of glass beads (BioSpec Products) in a 50 mL conical tube. 10 mg G4-6 was added and mixed overnight at 4˚C. The mixture was then centrifuged at 25,000 rpm for 30 min using a TA25.50 rotor (Beckman). The supernatant was then recirculated on a 5 mL Ni-NTA column (Qiagen) in a closed loop for 1.5 h using a peristaltic pump (Biorad, EP-1 EconoPump). The Ni-NTA column with bound ACTC-G4-6 complex was then washed with 30 mL of Buffer A containing 50 mM KCl and 40 mL of Buffer A containing 50 mM KCl and 20 mM Imidazole. A 1 mL HiTrap DEAE Sepharose FF column (GE Healthcare Life Science)

```
ACTC_BOVIN      MCDDEETTALVCDNGSGLVKAGFAGDDAPRAVFPSIVGRPRHQGVMVGMGQKDSYVGDEA
ACTC_HUMAN      MCDDEETTALVCDNGSGLVKAGFAGDDAPRAVFPSIVGRPRHQGVMVGMGQKDSYVGDEA
                ************************************************************

ACTC_BOVIN      QSKRGILTLKYPIEHGIITNWDDMEKIWHHTFYNELRVAPEEHPTLLTEAPLNPKANREK
ACTC_HUMAN      QSKRGILTLKYPIEHGIITNWDDMEKIWHHTFYNELRVAPEEHPTLLTEAPLNPKANREK
                ************************************************************

ACTC_BOVIN      MTQIMFETFNVPAMYVAIQAVLSLYASGRTTGIVLDSGDGVTHNVPIYEGYALPHAIMRL
ACTC_HUMAN      MTQIMFETFNVPAMYVAIQAVLSLYASGRTTGIVLDSGDGVTHNVPIYEGYALPHAIMRL
                ************************************************************

ACTC_BOVIN      DLAGRDLTDYLMKILTERGYSFVTTAEREIVRDIKEKLCYVALDFENEMATAASSSSLEK
ACTC_HUMAN      DLAGRDLTDYLMKILTERGYSFVTTAEREIVRDIKEKLCYVALDFENEMATAASSSSLEK
                ************************************************************

ACTC_BOVIN      SYELPDGQVITIGNERFRCPETLFQPSFIGMESAGIHETTYNSIMKCDIDIRKDLYANNV
ACTC_HUMAN      SYELPDGQVITIGNERFRCPETLFQPSFIGMESAGIHETTYNSIMKCDIDIRKDLYANNV
                ************************************************************

ACTC_BOVIN      LSGGTTMYPGIADRMQKEITALAPSTMKIKIIAPPERKYSVWIGGSILASLSTFQQMWIS
ACTC_HUMAN      LSGGTTMYPGIADRMQKEITALAPSTMKIKIIAPPERKYSVWIGGSILASLSTFQQMWIS
                ************************************************************

ACTC_BOVIN      KQEYDEAGPSIVHRKCF
ACTC_HUMAN      KQEYDEAGPSIVHRKCF
                *****************
```

Figure 7. Protein sequence alignment comparing human and bovine ACTC using BLAST. The α-cardiac actin of bovine (ACTC_BOVIN) and humans (ACTC_HUMAN) share 100% sequence identity.

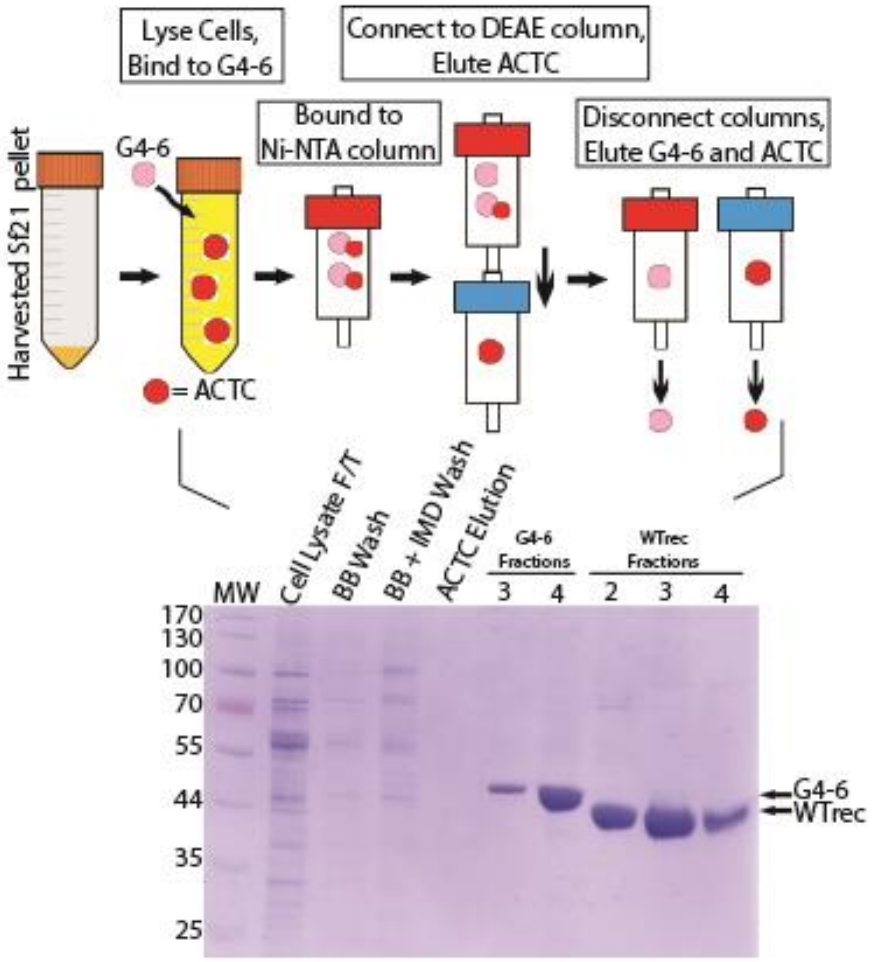

Figure 8. Purification of recombinant ACTC. Infected *Sf*21 pellets are lysed and His-tagged G4-6 is added to bind to ACTC. The ACTC-G4-6 complex is the loaded onto a Ni-NTA column. A DEAE column is added line with the Ni-NTA column and buffer is injected through the system that dissociates ACTC from G4-6, binding to the DEAE column. Both columns are detached and developed with buffers to elute G4-6 and ACTC, respectively. The progress of purification samples are run on a 10% SDS-PAGE stained with Coomassie Blue to show the actin protein as whole cell lysate, after recirculating through Ni-NTA column (Cell Lysate F/T), and elutions from washing with Binding Buffer followed by ACTC elution wash to release Actin from Ni-NTA column and to bind to DEAE column in tandem. The fractions showed successful G4-6 elution from the Ni-NTA column and actin recombinants from the DEAE column separately.

was attached in line with the Ni-NTA column and 40 mL of Buffer D (50 mM KCl, 10 mM Tris, pH 8.0, 0.2 mM EGTA, 0.2 mM PMSF, 0.5 mM $MgCl_2$, 0.2 mM ATP, 2 mM β-mercaptoethanol) was flushed through the system to dissociate ACTC from the G4-6 on the Ni-NTA column and then bind to the DEAE column. The DEAE column was then disconnected from the Ni-NTA column and is left aside. Buffer E (50 mM KCl, 10 mM Tris, pH 8.0, 0.2M imidazole, 5 mM $CaCl_2$, 1 mM PMSF, 1 mM ATP, 2 mM β-mercaptoethanol) was then injected through the Ni-NTA column to elute the His-tagged G4-6 and 1.5 mL fractions were collected. His-tagged G4-6 were pooled and dialyzed into Buffer G (2 mM Tris, pH 8.0, 0.2 mM $CaCl_2$, 0.2 mM ATP, 0.5 β-mercaptoethanol, 0.002% NaN_3) to be reused again in future preps. The Ni-NTA column was disconnected from the peristaltic pump and was replaced with the 1 mL DEAE column. Buffer F (10 mM Tris, pH 8.0, 0.2 mM $CaCl_2$, 0.2 mM ATP, 0.2 mM PMSF, 0.2 mM β-mercaptoethanol, 0.3 M KCl) was then run through the system to elute bound ACTC protein. 1 mL fractions were run on 10% SDS-PAGE to verify the presence of pure ACTC and the progress of purification.

The fractions containing the highest concentration of ACTC protein were mixed with troponin and tropomyosin at a molar ratio of 7:3:3 ACTC:Tn:Tm and dialyzed overnight against 500 mL of Buffer H (20 mM imidazole, 10 mM KCl, 2 mM $MgCl_2$, 1 mM DTT, 2 mM ATP, and 1 mM EGTA). The purified ACTC variant proteins were kept on ice at 4˚C for up to a week.

2.4.5 Purification of Troponin and Tropomyosin

The protocol for troponin and tropomyosin purification was adapted from Tobacman and Adelstein (1986), and Greaser and Gergely (1971). Bovine hearts were obtained from the Animal Biosciences Department at the University of Guelph. Approximately 450 grams of ventricular tissue were excised and grounded. The ground muscle was then blended with a solution containing 0.5 M boric acid, 50 mM sodium borate, 2 mM DTT, and 0.125 M KCl, and 0.2% Triton X-100. The suspension was centrifuged and washed in this buffer 4 times. The suspension was then washed with 6 L of 95% ethanol and centrifuged. The mince from the pellets was then bound up in cheese cloth and dipped into 3L of anhydrous ethyl ether 2 times. Finally, the mince was spread over filter paper and dried overnight in a fume hood. The dried ether powder was then weighed and stored at -80 ˚C for future use.

For troponin and tropomyosin purification, the dry ether powder was extracted overnight in 300 mL of solution containing 10 mM Tris, pH 8.0, 1 mM DTT, 1 M KCl, 0.01% NaN_3, 5 mg/L of TPCK and TLCK, and 0.3 mM PMSF. The mixture was centrifuged to obtain a clear supernatant. Solid ammonium sulfate was added to the supernatant to 30% saturation to precipitate actin. Following centrifugation, additional ammonium sulfate was added to the supernatant to reach 45% saturation. The solution was then centrifuged. The resulting pellet contained troponin while the supernatant contained tropomyosin. The pellet of the 45% ammonium sulfate cut was homogenized and dialyzed against 2L of 10 mM Tris, pH 8.0, 1 mM DTT, 0.01% NaN_3, 5 mg/L of TPCK and TLCK, and 0.3 mM PMSF. Further purification of troponin was done with a MonoQ 10/10 anion exchange column (GE Healthcare). Troponin was eluted with a 0-0.4

M NaCl gradient for 80 minutes at a rate of 1 mL/min and then 0.4 M-1 M NaCl gradient for 20 minutes at a rate of 1 mL/min. Elution fractions absorbing at OD 280 on the chromatogram were run on 12% SDS-PAGE. Fractions containing troponin were pooled and dialyzed in a solution containing 10 mM Tris, pH 8.0, 2 mM DTT, and 0.01% NaN_3. The concentration of troponin was determined via absorbance as outlined in **2.2.1**.

To purify tropomyosin, solid ammonium sulfate was added to the 45% ammonium sulfate cut supernatant to 65% saturation. The pH of the solution was lowered to 5 with 1 M HCl and centrifuged to obtain a pellet. The pellet was homogenized and dialyzed against a solution containing 50 mM Tris- pH 8.0, 0.01% NaN_3, 5 mg/L TPCK and TLCK, and 5 M urea. The dialyzed solution was then loaded onto a 25 mL Q Sepharose Fast Flow anion exchange column and developed overnight with a gradient of zero to 0.6 M NaCl at a rate of 0.33 mL/min. Elution fractions absorbing at OD280 on the chromatogram were run on 12% SDS-PAGE and fractions containing tropomyosin were pooled and dialyzed in a solution containing 10 mM Tris, pH 8.0, 1 mM DTT, and 0.01% NaN_3. Tropomyosin concentrations were determined via absorbance as outlined in **2.2.1**.

2.4.6 Data Management Plan for Protein Purification

Each SDS-PAGE was scanned onto Canon MP Navigator and saved as jpeg files onto Haidun Liu's flash drive. The scanned SDS-PAGE photo was processed on Haidun Liu's laptop where it was cropped and labeled in Adobe Illustrator. The labeled gels were then copied and pasted onto Adobe Photoshop and saved as png files with transparent background. All raw data, meta-data, and final data were saved in Haidun Liu's laptop and then uploaded onto the Dawson Lab Confluence page for archiving.

2.7 Actin-activated myosin ATPase assay

The interactions between purified ACTC variant proteins and full-length myosin were investigated using an actin-activated myosin ATPase assay (Trybus, 2000). This assay measures the amount of inorganic phosphate (P_i) released from the ATPase activity of myosin stimulated by the presence of actin. The P_i released interacts with the molybdate in the colour developing solution creating phosphomolybdate. The reduction of phosphomolybdate by ferrous sulfate creates a blue product, which can be measured colorimetrically.

There were two variations of the myosin ATPase assay used in this thesis: 1) to determine Michaelis-Menten curve of myosin ATPase activity using varying concentrations of unregulated ACTC variant proteins, and 2) to generate pCa curves of myosin ATPase activity at a constant concentration of ACTC variant proteins.

2.7.1 Myosin ATPase Michaelis-Menten Curves

Actin was mixed in a 1000:1 molar ratio with gelsolin and incubated at room temperature for 10 min to control actin filament viscosity. Polymerization was induced using a 10 x Assay Buffer (10 x AB: 750 mM KCl, 100 mM imidazole, pH 7, 10 mM DTT, 10 mM EGTA, 10 mM $MgCl_2$, and 10 mM NaN_3) and incubated at room temperature for 30 min. A 2x F-actin stock for each actin concentration was made by diluting the original F-actin stock in 1 x AB and Mg-ATP (2 mM) mix. A 2x myosin working solution was made using 1x AB to 0.25 mg/ml myosin.

Two 96-well plates were utilized, one for the reaction and phosphate standards and another contains 45 μL of stop solution (60 mM EDTA, pH 6.5, 6.6% SDS). A

schematic of the reaction and phosphate standard plate is shown in **Figure 9A** where the bottom two rows contain the phosphate standards ranging from 0.05 mM – 2 mM KH_2PO_4. These standards are required to create a standard curve for each assay performed. The top two rows contain the reaction wells set up in triplicate for each actin concentration. In these reaction wells, 100 µl of F-actin was mixed with 100 µL myosin, giving a final actin concentration in each triplicate wells ranging from 0-20 µM, respectively. The reaction started after the addition of 100 µl of myosin to the wells containing actin. Every 10 min after the start of the reaction, 45 µl of solution was removed from the reaction plate and mixed with 45 µl of stop solution in the stop plate to prevent further P_i production. To visualize the colour, each well received 200 µl of colour-developing solution (0.5% ferrous sulfate, 25% of 2% ammonium molybdate in 4 N H_2SO_4. P_i product appeared blue upon the addition of the colour-developing solution, which was measured colourimetrically at 750 nm for quantification.

2.7.2 Myosin ATPase pCa curves

Regulated thin filaments (RTFs) were made by mixing actin with troponin and tropomyosin in a molar ratio of 7:3:3 (22.2 uM Actin: 9.43 uM Tn: 9.43 uM TM), respectively. RTFs and F-actin were then dialyzed extensively into assay base buffer (1x ABB) containing 20 mM imidazole, 10 mM KCl, 2 mM $MgCl_2$, 1 mM DTT, 2 mM ATP, and 1 mM EGTA. A 2x HMM working solution was also made using 1x ABB without ATP to 0.25 mg/mL. 90 uL of RTFs and F-actin was then aliquot into different micro centrifuge tubes each 10 uL of 10x ABB buffer containing various pCa.

One 96-well plate was utilized that contains the phosphate standards as performed

in **2.7.1**, and the reaction wells containing each pCa condition in triplicate, as seen in **Figure 9B**. In the reaction wells, 25 uL of RTFs-pCa mixture was mixed with 25 uL of HMM, giving a final RTF concentration of 20 mM and 0.125 mg/mL of HMM in each triplicate. The reaction was initiated by the addition of HMM to the reaction wells. After 40 min of incubation, 50 uL of stop solution was added to the wells to cease reactions and a colour-developing solution was added to colorimetrically quantify the amount of P_i products as performed in 2.7.1.

The ATPase rate of myosin stimulated at varying pCa was calculated on a customized excel sheet containing the original absorbance values from the plate reader and converted values. The average background absorbance from the wells containing water (W) was subtracted from the average absorbance recorded for each phosphate standard concentration. Plotting the average absorbance against the phosphate standard concentrations generated a standard curve. The rate of P_i released was calculated for each pCa condition by dividing the slope of the standard curve and accounting for the y-intercept. Due to high basal activity at low pCa, the ATPase rate at pCa 10 was subtracted from the rate at each pCa. To easily compare and view the pCa_{50} for each RTF variant, each pCa condition was compared to the activity at pCa 4.5 to obtain % maximum activity. A sigmoidal graph of pCa vs. % maximum activity was made on GraphPad Prism 6 (San Diego, California) and a log (agonist) vs. response-variable slope was fitted to the data. The goodness of fit and the pCa_{50} was obtained from the graph. A Dunnett's test was used to determine statistical differences between ACTC variants and WTrec using SPSS version 24 (Richmond, CA) program.

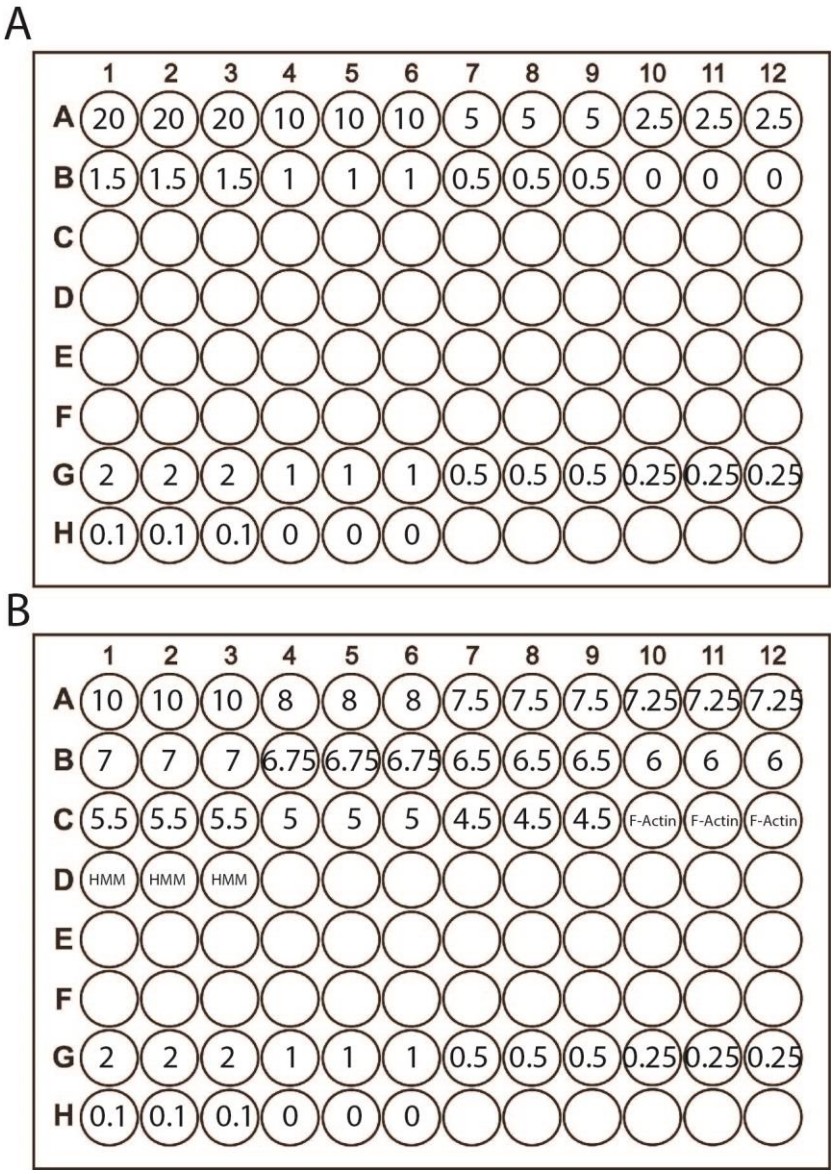

Figure 9. ATPase Assay 96-well plate setup. **A**. Myosin ATPase Michaelis-Menten curves 96-well plate setup consist of reaction wells at the top two rows with 100 uL of F-actin at concentrations varying from 20 uM to 0 uM. Bottom two rows consist of the phosphate standards with concentration ranging from 2 mM to 0 mM. The reaction starts by the addition of myosin diluted to final concentration of 0.125 mg/mL in each well. At 10 min intervals, 45 uL of solution is taken out from reaction and mixed into stop solution in a separate 96-well plate (not shown). **B**. Myosin ATPase pCa curves 96- well plate setup consist of reaction wells at the top 4 rows with 25 uL of RTFs and F-actin in pCa 10 to pCa 4.5. Negative controls consist of individual proteins and 1x ABB buffer. The reaction is initiated upon addition of 25 uL of HMM to final concentration of 0.125 mg/mL in each well. At 40 min, 50 uL of stop solution is added to the reaction.

2.7.3 Data Management Plan for Myosin ATPase assays

Raw text files of the absorbance values obtained from the plate reader were initially saved on Haidun Liu's USB flash drive. The raw data was processed and analyzed with Microsoft Excel. Analyzed data and values were graphed on GraphPad Prism 6 (San Diego, California) and saved as pzf and jpeg formats onto the laptop. All the raw data, meta-data, and final data were uploaded onto Haidun Liu's Confluence page.

2.8 *In vitro* Motility Assay

The *in vitro* motility assay protocol used in my work was adapted from Toyoshima et al. (1987). HMM was further purified through a process called "deadheading" to obtain active HMM. Deadheading was done by binding actin filaments to HMM in the absence of ATP followed by centrifugation at 95,000 rpm in a Beckman-Coulter TLA110 rotor for 15 min to obtain the insoluble acto-HMM pellet. The pellet was thoroughly resuspended in assay buffer (25 mM KCl, 25 mM imidazole, pH 7.5, 10 mM DTT, 4 mM $MgCl_2$, and 1 mM EGTA). Upon adding 2 mM ATP to the re-suspended pellet, HMM is released from the F-actin and the solution is immediately centrifuged at 95,000 rpm in a Beckman-Coulter TLA110 rotor for 10 min to obtain active HMM in the supernatant (**Figure 10**).

Nitrocellulose-coated coverslips and two sided tape were used to create flow cells on microscope slides where proteins were flowed in and incubated for 2 min for protein binding and buffer exchanges. Deadheaded HMM diluted to 0.125 mg/mL in assay buffer was injected first into the flow cell. Bovine serum albumin (BSA) diluted to 1 mg/mL in

assay buffer was injected into the flow cell to block the areas on the nitrocellulose coverslip where HMM did not bind. Assay buffer was then injected to the coverslip to wash out any proteins that did not bind to the nitrocellulose coverslip. Prior to binding, ACTC proteins variants (naked and/or regulated thin filaments) were fluorescently labeled with rhodamine-phalloidin at a 1:2 molar ratio with actin proteins. The fluorescently labeled actin filaments were diluted to ~0.1 uM and bound to HMM in the nitrocellulose coverslip. The flow cell was then washed with assay buffer prior to the addition of motility buffer (MB) (For unregulated actin, motility buffer (MB_{UN}) consisted of 25 mM KCl, 25 mM imidazole, pH 7.5, 10 mM DTT, 4 mM $MgCl_2$, 1 mM EGTA, and 2 mM ATP. For regulated thin filaments, motility buffer (MB_{RTF}) consisted of pCa 4.5-10, 25 mM KCl, 25 mM imidazole, pH 7.5, 10 mM DTT, 4 mM $MgCl_2$, 1 mM EGTA, and 2 mM ATP). An oxygen-scavenging system (25 ug/mL glucose oxidase, 45 ug/mL catalase, and 1% glucose) was used to prevent photobleaching of fluorescently labeled actin filaments. The flow cell was then inverted onto a Zeiss Axiovert 200M (Zeiss, Jena, Germany) microscope and actin proteins were visualized at 100x oil-immersed magnification using the Texas Red (510 nm) filter (**Figure 10**).

Movements of filaments were captured using a digital CCD ORCA-R2 C10600 camera (Hamamatsu, Middlesex, NJ) controlled by Volocity 6.3 software at a frame rate of 2.48 frames/second. Three movies at different location of the nitrocellulose coverslip were captured to provide a good representation of average movements.

2.8.1 Manual Tracking of *in vitro* Motility Assay data

The manual tracking procedure for RTF and unregulated F-actin filaments was performed similarly to Fraser and Martson (1995). 20 ACTC variants single filaments

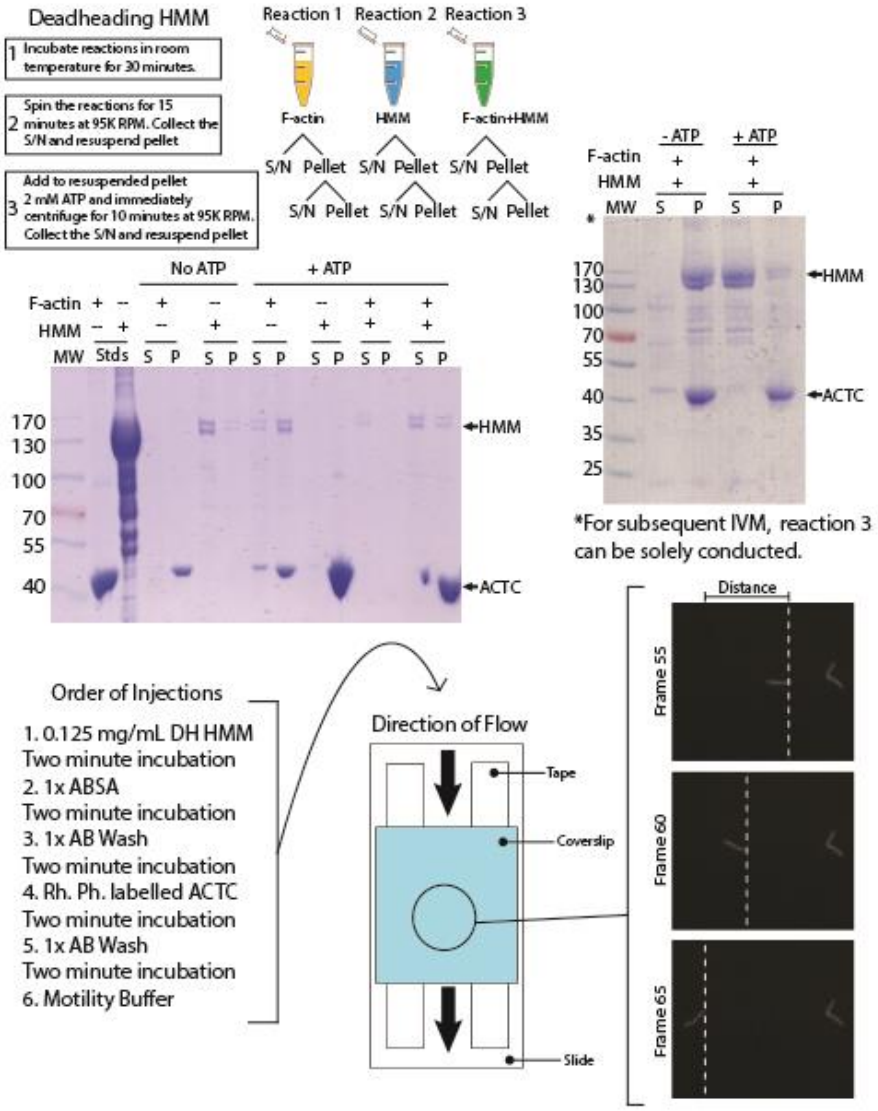

Figure 10. **The process of *in vitro* motility assay.** HMM is deadheaded by: binding to actin in the absence of ATP, centrifuging the reaction to obtain the pellet containing acto-HMM, resuspending the pellet with assay buffer and adding 2 mM ATP, and centrifuging the second reaction to obtain the supernatant containing the released HMM. Samples for the reaction are run on a 10% SDS-PAGE containing myosin and actin control samples. A microscope slide with a nitrocellulose coverslip constitutes a flow cell where proteins and buffers are injected in the following order: deadheaded HMM, BSA, Assay buffer, rhodamine-phalloidin labelled actin, Assay buffer, and finally motility buffer containing ATP (also calcium for regulated thin filaments). The flow cell is inverted onto an epifluorescence microscope with a Texas Red filter (510 nm). Filaments moving in a linear pattern are analyzed using ImageJ (manual tracking) and/or FAST (automatic tracking) to find average velocities.

moving in a linear pattern for at least 6 frames were selected. Each filament's length moved was tracked using Image J 1.47v and recorded on a customized Excel spreadsheet containing input of individual filament's coordinates, length track in pixels, frame rate displacement, and individual filament's velocities. The calibration of 89.5 nm/pixel was used to determine the total distance moved by each filament. In video analysis of RTFs, the average velocity of each pCa condition was obtained and input on GraphPad Prism 6 (San Diego, California) to be graphed. A one site specific binding with Hill slope was fitted to the data to obtain a sigmoidal curve. The goodness of fit and the pCa_{50} was obtained from the graph.

2.8.2 Automated Tracking analysis of *in vitro* Motility Assay data with FAST

An automatic tracking system called FAST (Fast Automated Spud Trekker) was also used to analyze all the filaments within a movie (Aksel, et al. 2015). FAST completes the analysis of a 30 frame *in vitro* motility movie in less than 30 s providing detailed output. Maximum velocity (plateau and top 5%) is estimated from a distribution that is filtered with respect to filaments with fluctuating velocities. Filtered and unfiltered distributions are displayed in FAST output side by side to show the effect of filtering. In addition, the percentage of stuck filaments is also displayed to assess the quality of motility in unloaded conditions. Finally, FAST also displays the mean of velocity distribution and top 5% velocities change with decreasing tolerance in filtering.

2.8.3 Data Management Plan for *in vitro* Motility Assay

Upon acquiring videos from the microscope using the Zeiss Axiovert 200M microscope (Zeiss, Jena, Germany) and velocity software, videos were saved as tiff files under a sub-folder in the Confocal Image Mac Computer. The whole folder was uploaded to Haidun Liu's External Hard drive (WD, 2 TB) to be stored. The folder was also copied and transferred to the Dawson Lab iMac Computer in the support room of 2203A for additional backup. Videos were analyzed using Image J and a customized Microsoft Excel sheet. The length of path filaments taken from Image J and
Excel sheet data were saved on Haidun Liu's laptop and external hard drive. Analyzed data and values were graphed on GraphPad Prism 6 (San Diego, California) and saved as pzf and jpeg format onto the laptop. All the metadata and final data were uploaded onto Haidun Liu's Confluence page.

Chapter 3 - Results

3.1 ACTC purification from *Sf*21/Baculovirus system

ACTC variants proteins were extracted from infected *Sf*21 insect cell lysates and purified by affinity chromatography (**Figure 11A**). Recombinant ACTC preparations yielded between 2.20 to 4.25 mg of purified protein from a 500 mL insect cell culture (**Figure 11B**) using the method described in Section **2.4.4**. Using Kruskal-Wallis analysis for non-parametric data to compare all ACTC variant protein yield against WTrec protein yields, I found no significant differences for E99K and F90Δ ($p>0.05$); there was significantly more protein yield with H88Y ($p= 0.009$) and R95C ($p= 0.048$).

3.2 Duty Ratio of Actomyosin with ACTC variants

The duty ratios of unregulated WTrec. R95C, E99K, H88Y, and F90Δ ACTC thin filaments were calculated by measuring the v_0 from *in vitro* motility assays, and k_{app} of myosin from ATPase-Michaelis-Menten curves. These values were entered into the equation for determining the duty ratio of myosin described in section **1.9**.

From the results of *in vitro* motility assay, there was a significant decrease ($p=0.019$) between WTrec (v_o =1.99 um/sec) and E99K (v_o =1.25 um/sec) (**Figure 12A**). This decrease is consistent with previous studies (Dahari & Dawson, 2015; Debold et al., 2010); however, Dahari (2015) showed a larger difference between WTrec (v_o= 3.1 um/sec) and E99K (v_o= 1.8 um/sec). I also observed a significant increase ($p= 0.002$) between WTrec and F90Δ (v_o= 2.89 um/sec). Previous studies in the Dawson lab showed

A

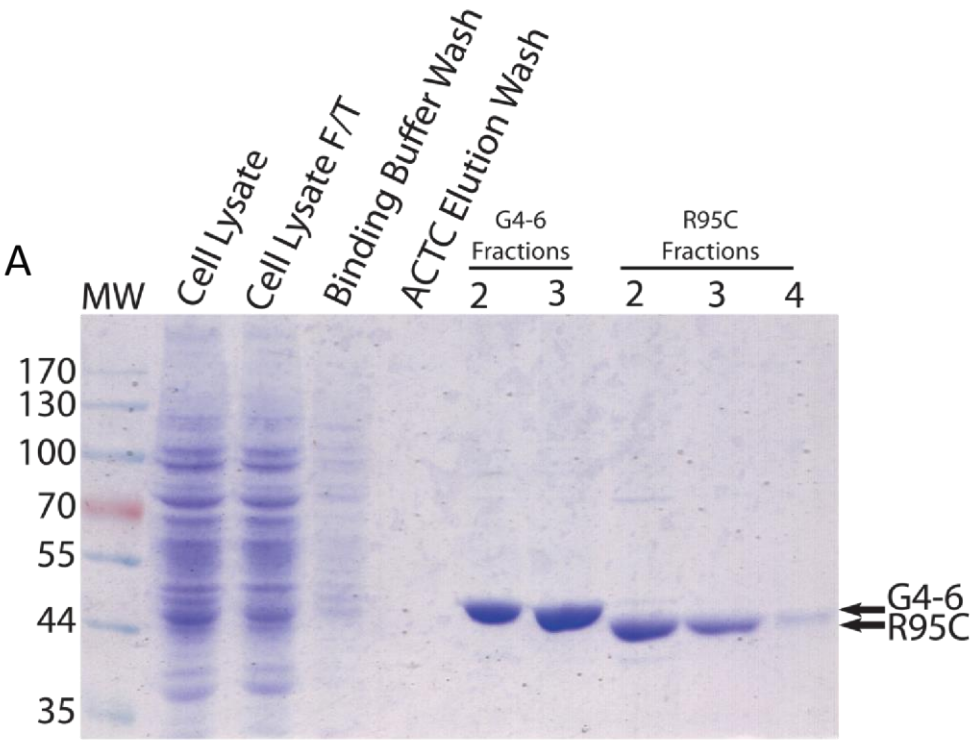

B

Mutant	$TCID_{50}$ (pfu/mL)	Virus Stocks	Average Yield (mgs)
WTrec ACTC	1.73×10^9	HL_E_01	2.39 ± 0.21, N= 22
F90Δ	1.00×10^9	HL_C_01	2.36 ± 0.14, N= 3
R95C	6.9×10^7	HL_B_01	3.14 ± 0.34, N= 14
H88Y	1.64×10^8	HL_D_01	4.25 ± 0.42, N= 3
E99K	1.48×10^9	HL_E_01	2.31 ± 0.31, N= 6

Figure 11. Protein purification of recombinant ACTC variants. A. The progress of purification on an 8% SDS-PAGE gel stained with Coomassie Blue for R95C showed the actin protein as whole cell lysate, after recirculating through Ni-NTA column (Cell Lysate F/T), and elutions from washing with Binding Buffer followed by ACTC Elution wash to release Actin from Ni-NTA column and to bind to DEAE column in tandem. The fractions showed successful G4-6 elution from the Ni-NTA column and actin recombinants from the DEAE column separately. **B.** The table shows information of each ACTC variants purification during the span of 2015-09-22 to 2016-07-18. The virus titre of each ACTC recombinant virus was determined using end point dilution outlined by O'Reilly *et al*., 1994 and and was infected into 500 mL volume with cell density of 1x10^6 cells/mL. No significant difference between WTrec ACTC (2.39±0.21, N=22) to E99K (p=0.77, 2.31±0.31 mg, N=6) and F90Δ (p=0.704, 2.36±0.14 mg, N=3). *There is signifcant difference between WTrec ACTC and R95C (p= 0.048, 3.14±0.34 mg, N=14) and H88Y (p= 0.009, 4.25±0.42 mg, N=3).

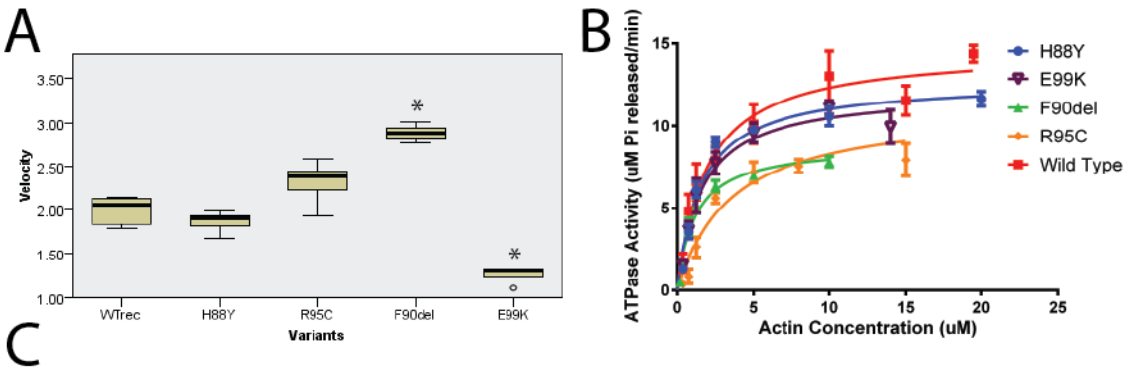

C

ATPase activities and *in vitro* motility velocities produced with pure

ACTC Variant	$k_{cat\ app}$ (/min)[1]	v_o (um/sec)[2]	Duty ratio, *r*	Relative *r*
WTrec	55.13	1.99 ± 0.02	0.593	1
E99K	47.08	1.25 ± 0.02	**0.807**	**1.35**
H88Y	*49.42*	1.84 ± 0.03	0.575	0.96
F90Δ	*34.40*	2.89 ± 0.06	**0.255**	**0.43**
R95C	*43.46*	2.23 ± 0.03	**0.417**	**0.70**

Duty ratios for each variant actomyosin complex were calculated with the expression: $r = \delta \cdot k_{cat} / v_o$, where δ is the step size of each myosin motor (taken as 5 nm).

[1] k_{cat} calculated using a myosin heavy chain MW of 486 kDa.

[2] under standard IVM ionic strength conditions (25 mM KCl)

Figure 12. Duty Ratio of ACTC variants WTrec, H88Y, R95C, and E99K.
A. Statistical Analysis (Kruskal-Wallis) of HCM ACTC variants' velocities obtained from in vitro motility assay. There were no significant differences between WTrec (N=9) to R95C (p>0.05, N= 11) and WTrec to H88Y (p>0.05, N= 9). There were significant differences betweenWTrec to F90Δ (*p<0.05, N= 8), and WTrec to E99K (*p< 0.05, N= 5). **B.**Michaelis-Menten curves of HCM ACTC variants. V_{max} of each HCM ACTC variants was obtained and were analyzed using the same statistical analysis. Comparing the ACTC variants' V_{max} obtained from myosin ATPase assay, there was no significant difference in comparing WTrec (N= 5) to E99K (p> 0.05, N= 3) and H88Y (p> 0.05, N= 6). There was significant difference in comparing WTrec to F90Δ (p<0.05, N=6) and R95C (p<0.05, N=5). **C.** Table compilation of k_{cat}, velocities, and duty ratios for each HCM ACTC variants. Relative duty ratios were calculated by comparing the duty ratios of HCM ACTC variants to WTrec. Duty ratio in bolded red font indicates ACTC variants with an increased duty ratio, E99K. Duty ratio in bolded blue font indicates ACTC variants with a decreased duty ratio, F90Δ and R95C. H88Y has a similar duty ratio to WTrec.

a decrease in F90Δ velocity (Anillo, 2015). It should be noted that in those studies a different purification method for the ACTC variants was employed that resulted in lower functioning proteins. However, the velocity obtained for F90Δ was similar (v_o= 2.55 um/s) to mine. In my study, ACTC proteins from insect cells were purified using a procedure that did not involve harsh detergents and resulted in active ACTC which gives me confidence in using them for my assays.

Michaelis-Menten plots of the myosin ATPase activity were performed by a project student, Mary Henein, under my supervision (**Figure 12B**). No significant differences between WTrec activity were seen compared to E99K and H88Y variants ($p>0.05$); there were significant decreases in comparing WTrec to F90Δ ($p<0.05$) and R95C ($p< 0.05$). Previous work in the Dawson Lab showed an increase in the myosin ATPase rate between WTrec and E99K (Dahari & Dawson, 2015). More recent data from the lab also showed a significant decrease in R95C, H88Y, and F90Δ when comparing to bovine ACTC (Anillo, 2015).

Using velocity data from *in vitro* motility assays, myosin ATPase rates, and the assumption of a myosin step size 5 um, duty ratios were calculated and compared between ACTC variants (**Figure 12C**). Using the WTrec's duty ratio as a comparison, E99K has an increased relative duty ratio of 1.35, while H88Y, F90Δ, and R95C have lower relative duty ratios of, 0.96, 0.43, and 0.70, respectively. Previous study from the Dawson lab had shown an increased duty ratio of E99K and R95C and a decreased duty ratio of H88Y and F90Δ (Anillo, 2015; Dahari & Dawson, 2015).

3.3 Comparison of WTrec and Bovine cardiac RTFs Curves

Data from individual biological replicates (N) of each ACTC variant were compiled and graphed using a log-response four parameter fitting algorithm on GraphPad Prism 6 (San Diego, California) to obtain the average pCa_{50} and V_{max}. RTFs containing WTrec and tissue-purified bovine ACTC RTF were investigated to compare tissue-purified and recombinant proteins in our system. For my pCa curves, data are presented in two forms: 1) as a percentage of the dynamic range (%DR), and 2) as the absolute values of the activity being measure. The %DR representation allows us to more intuitively compare pCa_{50} values at a glance, while the absolute values provide a picture of differences in the activities themselves that might be a result of mutations.

3.3.1 Comparing WTrec to Bovine RTF- Myosin ATPase- pCa Curves

Examining %DR (**Figure 13A1**), the WTrec curve (pCa_{50}= 7.11, N= 4) is shifted to the left compared to bovine RTFs (pCa_{50}= 6.42, N= 5). Looking at the absolute activity (**Figure 13, A2**) , the pCa_{50} difference between WTrec and bovine RTF is more pronounced; however, bovine RTFs have a higher maximal ATPase activity (Vmax= 16.26 uM/min) compared to WTrec RTFs (11.92 uM/min).

3.3.2 Comparing WTrec to Bovine RTF- IVM Method A

In the *in vitro* motility assay method A (% filaments motile), there is only a slight difference between WTrec (pCa_{50}= 6.66, N= 3) and Bovine RTFs (pCa_{50}= 6.78, N= 8) in the %DR (**Figure 13B1**). Bovine RTFs have a higher basal number of filaments moving at high pCa (Y_{min}= 6.27 filaments) than WTrec (Y_{min}= 1.24 filaments). Similarly, bovine

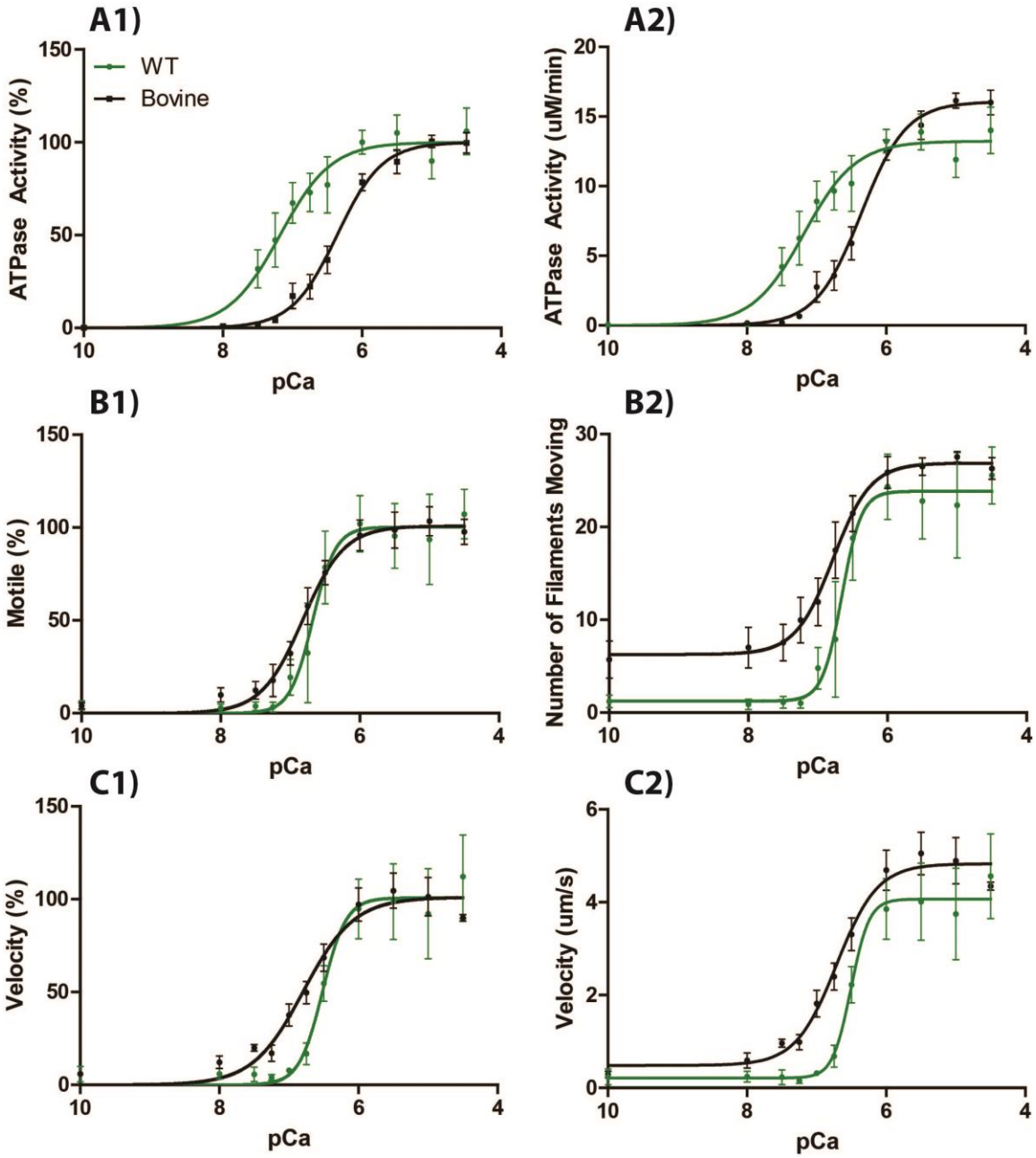

Figure 13. Comparison of WTrec and Bovine RTFs . Data obtained from myosin ATPase and in vitro motility assay for WTrec and bovine ACTC was graphed in GraphPad Prism 6 (San Diego, California) using a log response-four parameter fitting, thereby showing the absolute range (A2, B2, and C2). To visualize any disparity between the ACTC variants, data was zeroed and normalized from the line of best fit to obtain a %DR (A1, B1, and C1). Briefly, there is a large disparity in pCa_{50} and V_{max} between WTrec and bovine ACTC in the myosin ATPase assay (A1 and A2). In both methods of *in vitro* motility assay, Bovine ACTC has higher basal activity and V_{max} compared to WTrec ACTC in the dynamic fit range (B2 and C2).

RTFs have a higher maximum number of filaments moving at low pCa than WTrec (Y_{max}= 26.88 and 23.85 filaments, respectively).

3.3.3 Comparing WTrec to Bovine RTF- IVM Method B

Looking at the %DR (**Figure 13C1**) of *in vitro* motility assay method B (examining the velocity of the filaments), WTrec RTFs show has a pCa_{50} shift to the right of bovine RTFs (pCa_{50}= 6.51, N=3 and 6.71, N=6 respectively), similar to the shift seen with % motile filaments in the same assay. Similar to the previous graphs (**Figure 13B2 and C2**), bovine RTFs (Y_{min}= 0.48 μm/sec, Y_{max}= 4.83 μm/sec) have a slightly higher basal velocity and a higher maximal velocity compared to WTrec RTFs (Y_{min}= 0.21 μm/sec, Y_{max}= 4.07 μm/sec).

3.4 Comparison of ACTC concentration methods

We saw unexpected differences in ACTC function between bovine ACTC and WTrec RTFs, especially in the myosin ATPase-pCa curves. To examine the potential cause of these differences, we explored the different methods used to determine the concentrations of the ACTC proteins: bovine ACTC was determined spectrophotometrically at OD_{290} with an extinction coefficient of 0.62 cm^{-1}, while recombinant ACTC proteins are determined using a Bradford assay. The bovine ACTC used in experiments yielded a concentration of 4.58 ± 0.02 mg/mL determined spectrophotometrically. In the Bradford Assay, the same bovine ACTC sample yielded concentrations ranging from 1.92 ± 0.036 to 7.97 ± 0.35 mg/mL (**Table 1**). Upon

Table 1. Bovine ACTC concentration values obtained from an OD of 290 nm and 595 nm. In one method, bovine ACTC sample's absorbance was measured using DU800 spectrophotometer in at an OD of 290 nm. With the same bovine ACTC, it was first serial diluted from 2x to 128x and pipetted onto a 96 well plate in triplicate. After adding Bradford reagent, the absorbance of each sample was read at 595 nm.

	Absorbance at 290 nm	Absorbance at 595 nm				
	Conc. (mg/mL)	DL	Conc. (mg/mL)	DL	Conc. (mg/mL)	Average (mg/mL)
Bovine ACTC	**4.58 ± 0.02**	2x	1.92 ± 0.036	32x	8.20 ± 0.21	**6.19 ± 0.87**
		4x	3.38 ± 0.069	64x	8.85 ± 0.13	
		8x	5.57 ± 0.024	128x	7.97 ± 0.35	
		16x	7.27 ± 0.17	100x	6.38 ± 0.41	

In both methods, the baseline absorbance was zeroed against G-Buffer (2 mM Tris, pH 7.5, 0.2 mM $CaCl_2$, 0.2 mM ATP, 0.5 mM β-mercaptoethanol, and 0.002% NaN_3)

averaging the concentration from each dilution, the average concentration determined by Bradford Assay was 6.19 ± 0.87 mg/mL. This disparity from the two methods will affect the molar ratio of actin, Tn and TM and impact the activity of actomyosin complex (Eyk et al., 1997; Fraser & Marston, 1995). In my experiments, the concentration used for bovine ACTC was from spectrophotometer and the concentrations of ACTC variants purified from *Sf*21/baculovirus system was from Bradford Assay. Thus, data of RTFs with ACTC variants will be compared only to WTrec RTF and not to tissue-purified bovine RTFs.

3.5 Comparison of WTrec to R95C and E99K RTFs Curves

Since Bovine and WTrec RTF's show a difference in ATPase activity, I will be comparing R95C and E99K to only WTrec RTFs. These three ACTC proteins are purified with the same method outlined in section **2.4.4**.

3.5.1 Comparing WTrec to RTF variants- Myosin ATPase-pCa Curves

In comparing the %DR (**Figure 14A1**) of myosin ATPase- pCa, there is a small difference in pCa_{50} between WTrec, R95C, and E99K RTFs (pCa_{50}= 6.78, N= 4, 7.13, N=4, 7.20, N=5 respectively). Also, RTFs containing R95C and E99K ACTC variants show a lower maximal ATPase activity in the absolute range compared to WTrec (V_{max}=12.1, 9.66, and 14.4 μm/min, respectively).

3.5.2 Comparing WTrec to RTF variants- IVM Method A

In the *in vitro* motility assay (method A) of %DR, R95C and E99K pCa_{50} curves (pCa_{50}= 6.41, N= 4) and 6.29, N= 4, respectively) are shifted to the right relative to the WTrec curve (pCa_{50}= 6.66) (**Figure 14 B1**). In the absolute range, it is also noted that there are more basal filament movements at low pCa for E99K (Y_{min}= 4.89) than, WTrec (Y_{min}= 1.24), and R95C containing RTFs (Y_{min}= 0.51) (**Figure 14B2**).

3.5.3 Comparing WTrec to RTF variants- IVM Method B

Similar patterns are also observed in the *in vitro* motility assay method B in both %DR (**Figure 14C1**) and absolute velocities (**Figure 14C2**), with R95C (pCa_{50}= 6.24, N=4), E99K (pCa_{50}= 6.09, N=4), and WTrec (pCa_{50}= 6.52, N=3). In contrast, Debold et al. (2010) showed no differences in pCa_{50} between WTrec and E99K ACTC containing RTFs. Although there is no significant difference in the maximum velocity for WTrec, R95C, and E99K, there is a noticeable decrease in velocity with the variants (V_{max}= 4.10, 3.87, and 3.69 um/s, respectively). In comparison, ACTC variants WTrec, R95C, and E99K yield velocities of 1.99 ± 0.05, 2.32 ± 0.036, and 1.26 ± 0.04 um/sec, respectively (**Figure 12**). The increased velocity with RTFs is consistent with other studies (Fraser & Marston, 1995; Homsher et al., 2000). Another comparison between unregulated thin filaments and RTFs is that E99K have a lower velocity compared to WTrec in unregulated form (1.26/1.99 =0.63), but this difference is smaller in the regulated form (3.69/4.10= 0.9). Conversely, an increased velocity was seen with unregulated R95C

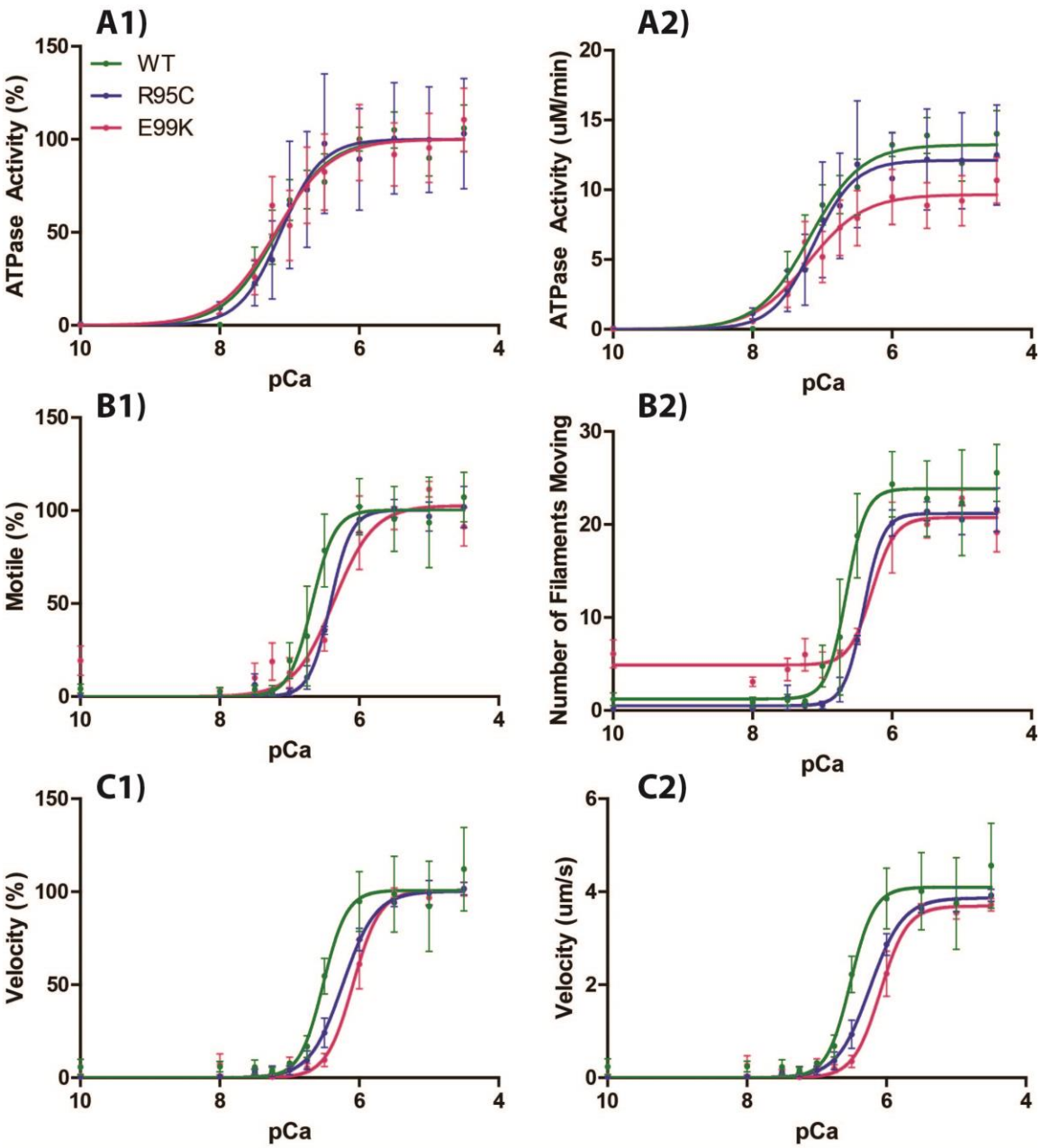

Figure 14. Comparison of R95C and E99K RTF to WTrec RTF. Similarily to Figure 13, the %DR (A1, B1, and C1) and absolute range (A2, B2, and C2) of each ACTC variant were fit using a log- response-four parameter. Briefly, there is no change between the ACTC variants in the myosin ATPase assay, but the standard error of mean is large for each data point (A1). In both methods of in vitro motility assay, R95C and E99K shifted the graph to the right of WTrec (B1 and C1).

compared to WTrec filaments (2.32/1.99= 1.17) with a decreased velocity in regulated form (3.87/4.1= 0.92).

3.6 Distribution of filament velocity

A vertical scatter plot was used to graph the velocity of single filaments at varying pCa to provide a picture of the variability in the single molecule measurements (**Figure 15**). 1,920 single filament velocities were graphed for WTrec, 3,729 filaments for bovine ACTC, 2,640 filaments for R95C, and 2,595 filaments for E99K, for a total of 10,885 individual filament velocities analyzed manually. Visually, WTrec, R95C, and E99K RTFs showed a pattern of having less dispersion at high pCa and more dispersion at low pCa. In contrast, Bovine RTFs showed high dispersion throughout each pCa.

3.7 pCa_{50} and V_{max} values from *in vitro* motility assay and myosin ATPase

The pCa_{50} and V_{max} values shown in **Table 2** differ from the values obtained from **Figures 13 and 14** based on how the data was processed. In **Figures 13 and 14**, each RTF ACTC variant pCa_{50} and V_{max} were calculated by inputting data from all biological replicate to obtain one fitted curve. Alternatively, the pCa_{50} and V_{max} of each RTF ACTC variant represented in **Table 2** were calculated by graphing individual biological replicates and averaging the resulting pCa_{50} and V_{max} values. In the second method, significant differences between pCa_{50} and V_{max} values can be calculated using a Dunnett's test.

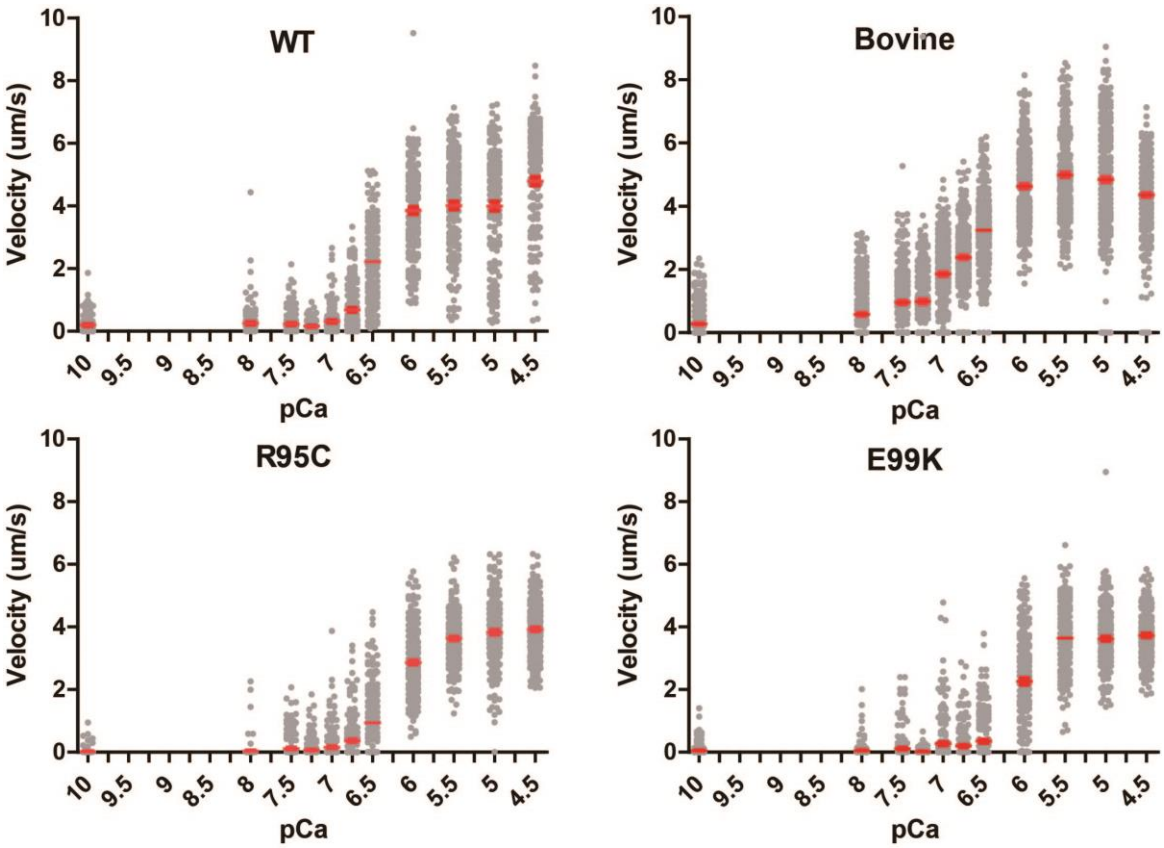

Figure 15. Distribution of individual RTF variant's velocity at varying pCa. Individual filament's velocity for each ACTC was compiled and was inputted into a vertical column-scatter graph using GraphPad Prism 6 (San Diego, California). Total number of filaments observed for each ACTC and biological replicates are as followed: WTrec (1920, N=3), Bovine (3729, N=6), R95C (2640, N=4), and E99K (2595, N=4).

Table 2. Data summary of RTF variants. A log vs. response-four parameter was fitted into each biological replicate to obtain the pCa_{50} and V_{max} values. The data was then inputted into SPSS (Richmond, CA) to obtain the average pCa_{50} and V_{max} and using post hoc Dunett's test to determine significant differences.

	Myosin ATPase		*in vitro* Motility Assay			
ACTC Variant	pCa_{50}	V_{max} (uM/min)	pCa_{50}	V_{max} (# Fil.)	pCa_{50}	V_{max} (um/s)
WTrec	7.31 ± 0.21	13.2 ± 0.82	6.64 ± 0.11	23.7 ± 4.1	6.51 ± 0.028	4.09 ± 0.87
Bovine	**6.39 ± 0.10**	15.9 ± 0.76	6.78 ± 0.087	27.1 ± 0.65	6.71 ± 0.050	4.85 ± 0.31
R95C	6.90 ± 0.24	12.4 ± 3.5	6.41 ± 0.033	21.3 ± 1.2	**6.24 ± 0.078**	3.84 ± 0.13
E99K	7.03 ± 0.20	9.93 ± 1.55	**6.23 ± 0.13**	21.6 ± 0.89	**6.07 ± 0.055**	3.65 ± 0.11

Red- significant difference between ACTC variants and WTrec ($p<0.05$)

Blue- significant difference between Bovine and WTrec ($P<0.05$)

With the myosin ATPase assasys, WTrec (N=4), bovine (N= 5), R95C (N= 4), and E99K (N= 4) resulted in pCa_{50} values of 7.31 ± 0.21, 6.39 ± 0.1, 6.9 ± 0.24, and 7.03 ± 0.020 respectively, with a significant difference between WTrec and bovine ACTC ($p=0.005$). Maximal activity for WTrec, bovine ACTC, R95C, and E99K were 13.2 ± 0.82, 15.9 ± 0.76, 12.4 ± 3.5, and 9.93 ± 1.55 μM/min, respectively. In comparison to V_{max} from myosin ATPase Michaelis-Menten curve, WTrec, bovine ACTC, R95C, and E99K (V_{max}= 14.2 ± 1.1, 14.9 ± 1.2, 11.2 ± 1.3, and 12.1 ± 0.70, respectively) were similar.

Two types of analysis were performed of the *in vitro* motility assay data. One type of analysis (Method A) observed whether the filaments are moving within the first 10 timepoints. In this analysis, WTrec (N=3), bovine ACTC (N= 8), R95C (N= 4), and E99K (N= 4) resulted in pCa_{50} of 6.64 ± 0.11, 6.78 ± 0.087, 6.41 ± 0.33, and 6.23 ± 0.013 respectively, with a significant decrease of E99K compared to WTrec ($p< 0.05$). Maximal filaments for WTrec, Bovine, R95C, and E99K were 23.7 ± 4.1, 27.1 ± 0.65, 21.3 ± 1.2, and 21.6 ± 0.89 filaments, respectively.

A second analysis of *in vitro* motility assays was done in the same manner to find the pCa_{50} and maximal velocity from a velocity-pCa graph. WTrec (N= 3), bovine ACTC (N= 6), R95C (N= 4), and E99K (N= 4) resulted in pCa_{50} of 6.51 ± 0.028, 6.71 ± 0.050, 6.24 ± 0.078, and 6.07 ± 0.055 respectively with significant differences between WTrec and E99K ($p=0.001$), and between WTrec and R95C ($p= 0.045$). The maximal activity for WTrec, Bovine, R95C, and E99K were 4.09 ± 0.87, 4.85 ± 0.31, 3.84 ± 0.13, and 3.65 ± 0.11 μm/sec, respectively.

3.8 Duty ratios of regulated actomyosin with ACTC variants

Duty ratios of regulated actomyosin were calculated in the same manner as in section 3.2 except for the molar concentration of myosin (**Table 3**). Soluble heavy meromyosin (HMM) was used instead of myosin full length for the purpose of limiting experimental errors (Sellers, 1999). Using the WTrec RTFs duty ratio as the comparison, bovine and R95C RTFs has a relative duty ratio of 1.02 and 1.00 respectively, while E99K have lower relative duty ratios of 0.85.

Table 3. Duty ratios of regulated thin filaments. Table compilation of k_{cat}, velocities, and duty ratios for each RTFs with HCM ACTC variants. Relative duty ratios were calculated by comparing the duty ratios of HCM ACTC variants to WTrec. Bovine and R95C has a relative duty ratios of 1.02 and 1.00, respectively. E99K has a lower relative duty ratio of 0.85.

ACTC Variant	$k_{cat\ app}$ (/min)[1]	v_o (um/sec)[2]	Duty ratio, r	Relative r
WTrec	37.0	4.09 ± 0.87	0.753	1.00
Bovine	44.5	4.85 ± 0.31	0.765	1.02
R95C	34.7	3.84 ± 0.13	0.753	1.00
E99K	27.8	3.65 ± 0.11	0.637	0.85

Duty ratios for each RTF variant actomyosin complex were calculated with the expression $r=\delta \bullet k_{cat}/v_o$, where δ is the step size of each myosin motor (5 nm).
[1]k_{cat} calculated using a heavy meromyosin MW of 350 kDa
[2]under standard IVM ionicstrength conditions (25 mM KCl)

Chapter 4 - Discussion

4.1 Production of pure recombinant ACTC proteins

The ACTC variant proteins (WTrec, R95C, F90Δ, H88Y, and E99K) were successfully expressed using our *Sf*21/Baculovirus system as seen in the Western and dot blots (**Figure 4**). Proteins were purified from insect cells using His-tagged protein G4-6 and affinity chromatography. In contrast to previous ACTC purification methodology that used harsh chemicals, I obtained pure ACTC proteins without the use of any harsh chemicals, which can be seen in the SDS-PAGE gels (**Figure 7**). The progress of purification gel was reproducible for all ACTC variant proteins purified.

4.2 Effects of Unregulated ACTC mutations on actomyosin interactions

The primary binding site of myosin is in subdomain 1 of actin, thus substitution mutations in this location may cause electrostatic changes, and affect the interaction of the actomyosin complex (Bookwalter & Trybus, 2006). I hypothesized that interactions of myosin with HCM-linked ACTC variants in subdomain 1 (R95C, H88Y, E99K, and F90Δ) would result in decreased duty ratios compared to WTrec ACTC. A decreased duty ratio correlates to decreased actomyosin interaction and lower contraction. Based on my results, E99K exhibited a higher relative duty ratio, H88Y exhibit no change in relative duty ratio, and R95C and F90Δ exhibited lower relative duty ratios (**Figure 12**). These results proved my hypothesis to be false.

4.2.1 Reasoning for change of duty ratio for E99K, R95C, F90Δ, and H88Y

The charge reversal of the E99K change would cause electrostatic repulsion of myosin and decrease the amount of cross-bridge formation. Although other studies showed an increase in K_m, our myosin ATPase data with E99K data (not shown) showed a decrease in K_m. Consistent with Bookwalter and Trybus (2006), a significant decrease in velocity was observed. However, they performed additional experiments such as rigor binding affinity and force assays, and showed that E99K resulted in an overall decrease in force capacity and weakened actomyosin interactions. Contrary to what I expected to see, the combination of decreased K_m and filament velocity in my experiments led to an increased duty ratio.

The myosin interactions of other subdomain 1 ACTC variants have not been reported in the literature. Consistent with my hypothesis, I saw decreased duty ratios for ACTC variants R95C and F90Δ. The change in duty ratio for R95C may be explained by the differences in properties of arginine and cysteine. Arginine is positively charged at neutral pH from the basic side chain. However, cysteine has a thiol (-SH) side chain and is not charged at neutral pH. The loss of a potential charge interaction with Arg-95 may account for the decreased binding between ACTC subdomain 1 and myosin, resulting in a lower duty ratio.

A decreased duty ratio was also observed for ACTC variant F90Δ. A deletion of phenylalanine in ACTC would lose possible aromatic-aromatic interactions (pi-stacking) that may occur with myosin. In addition, this phenylalanine residue is located at the end of the second helix in actin. Elimination of this residue may disrupt the secondary structure of the helix and the local conformation of the ACTC protein. This possible

change in the actin structure may be the reason for the decreased binding of myosin to ACTC.

The ACTC substitution mutation H88Y yielded no difference in duty ratio. Histidine has a basic side chain from the imidazole ring. In contrast, tyrosine has a hydrocarbon benzene ring, which is uncharged at neutral pH. The change of positive residues to a neutral residue may not be a large electrostatic difference compared to E99K ACTC substitution, or perhaps the presence of a ringed structure in the sidechain at this position is the most important factor.

Overall, my results disproved my hypothesis that all HCM linked ACTC variant will cause a decreased duty ratio. Other factors may contribute to changes in actomyosin activity, such as calcium sensitivity via the regulatory proteins troponin and tropomyosin.

4.3 Transition from unregulated thin filaments to RTFs

In contraction, the formation of cross-bridges not only involves the interaction of actin and myosin motor proteins; there are many other proteins that facilitate the process. Upon seeing varying myosin duty ratios for HCM ACTC substitution mutation, I hypothesized that the regulation of actomyosin by regulatory proteins may be altered in the presence of HCM-associated ACTC mutations. To test this hypothesis, I performed myosin ATPase assays and IVM assays using regulated thin filaments (RTFs) to generate pCa-activity and pCa-motility and velocity curves respectively. Any shift of the pCa curves, reported through pCa_{50} values, will report on how the activity is altered in response to calcium.

In comparison to the velocities of unregulated ACTC filaments in IVM, RTFs had higher velocities as observed in other studies (Clemmens & Regnier, 2004; A. M. Gordon, Homsher, & Regnier, 2000; Gordon et al., 1997; VanBuren et al., 2002). Interestingly, the exact mechanism for greater RTF velocity is still unknown. What is known is that regulatory proteins do not affect the hydrolysis of ATP on myosin, but they affect the cross-bridge cycle either by cross-bridge recruitment (Gordon et al., 2000; Homsher et al, 1996) or by modulation in the kinetics of cross-bridges (Swartz & Moss, 2001)

4.4 IVM and myosin ATPase pCa_{50} controls in relation to other studies

Previous studies of myosin ATPase and IVM have reported varying pCa_{50} between 5.9 - 7.1 in experiments using different proteins isoforms in RTFs (Fraser & Marston, 1995; Homsher et al., 1992; Lin et al., 1996; Robinson et al., 2002; Velden et al., 2003). Song et al. (2011) obtained a pCa_{50} for human cardiac RTFs of about 6.38 in IVM, measuring the fraction of RTF moving at varying pCa, similar to my Method A. Also expressing human ACTC in baculovirus insect cells for IVM assays, Debold et al. (2010) found the velocities of WTrec to have a pCa_{50} of 6.34. In two additional IVM studies that investigated bovine RTFs, the pCa_{50} was approximately 6.5 (Homsher et al., 1996; VanBuren et al., 2002). My pCa_{50} values from IVM are higher but they still fall within the range observed in the literature.

There are fewer studies of myosin ATPase at varying pCa compared to IVM, especially those that investigated ACTC protein. However, in studies that looked at RTFs

made with WT skeletal actin, a pCa_{50} of 6.44 was observed against myosin ATPase activity (Mirza et al., 2005). Another study used reconstituted RTF from porcine cardiac fibres to yield a myosin ATPase pCa_{50} of approximately 6.70 (Gomes et al., 2002). In comparison, my WTrec ACTC yielded a much larger pCa_{50} (7.31) while ACTC purified from bovine tissues yield pCa_{50} that is within the range in literature (6.39).

4.5 Other factors that affect thin filament motility

Although ionic strengths have been shown to affect actomyosin interactions, the exact mechanism is unknown (Gordon et al., 1973; Gulati and Podolsky, 1978). In IVM studies by Homsher et al. (1996, 1992), filament velocities were sensitive to ionic strength below 100 mM due to electrostatic screening caused by a high ionic strength, affecting the binding of myosin to actin. Gordon et al. (1997) showed that the electrostatic screening from increased ionic strength also affected the binding of calcium to troponin, and decreased the calcium sensitivity of RTFs. To prevent the phenomenon of electrostatic screening, studies have used low ionic strength. My thesis used the same low ionic strength salt solution as Debold et al. (2010) consisting of 25 mM KCl, 25 mM imidazole, 2 mM EGTA, 5 mM MgCl2, and 10 mM DTT. To avoid the influence of ionic strength and maintain consistency, the low ionic strength condition was used throughout all IVM assays.

One significant difference in IVM conditions between Debold et al. (2010) and my thesis is the addition methylcellulose in the motility buffer. Uyeda et al. (1990) saw lateral diffusion of filaments away from the surface with HMM, affecting the movement

of filaments. The introduction of methylcellulose solves this problem by adding viscosity to the solution and is sufficient to keep filaments of all length bound to the HMM surface. Furthermore, the presence of 0.9% methylcellulose allowed continuous movement of filaments and did not inhibit filament movements, but increased the sliding velocity. Future studies of Dawson Lab should consider the use of methylcellulose in IVM.

4.6 IVM and myosin ATPase pCa_{50} of WTrec and Bovine RTF

The pCa_{50} values obtained from IVM and myosin ATPase for WTrec and bovine RTF were not the same. Although there were no significant differences for IVM pCa_{50} values, there was a pCa_{50} difference of 0.14 for Method A and 0.20 for Method B. With myosin ATPase, there was a significant difference between WTrec and bovine RTFs (pCa_{50} difference= 0.92). Post-translational modification might differ between the ACTC expression system from *Sf*21 cells and bovine tissue-purified ACTC. Results from mass spectrophotometry analysis indicated that *Sf*21 cells are able to perform some of the post-translational modifications (**Figure 4**). It is speculated that the high expression rate may overwhelm the insect cells such that they do not properly modify the protein, resulting in lower posttranslational modifications of ACTC proteins (Bookwalter & Trybus, 2006; O'Reilly et al., 1994) and altered actin function. For example, acetylation of the N-terminus of actin facilitates actomyosin interactions in muscles (Terman & Kashina, 2014); perhaps a change in this modification occurs in the baculovirus system.

Another possible cause of the pCa_{50} difference between WTrec and ACTC purified from bovine cardiac is the inconsistent techniques used to determine

concentrations. The concentration of ACTC purified from bovine cardiac was determined spectrophotometrically at OD_{290}, while the concentration of recombinant ACTC expressed from *Sf*21 insect cells are determined via Bradford assay. As seen in **Table 2**, the ACTC concentration obtained by Bradford assay overestimated the concentration by 1.61mg/mL compared to the use of spectrophotometer at OD_{290}. This overestimation of bovine ACTC would affect the molar ratio with troponin and tropomyosin in the formation of RTFs. I speculate that the increased pCa_{50} (lower calcium sensitivity) is caused by the over saturation of troponin and tropomyosin complex. This excess of Tn-TM complex would interfere with the binding of actin and myosin by requiring more calcium to bind to troponin and free the inhibition of actin.

In retrospect, a Bradford assay was used to determine the concentration for WTrec yet the pCa_{50} was similar to literature values. The result of Bradford assay affecting the concentration of bovine and not WTrec ACTC may be due to the limited concentration sensitivity of the technique and the protein yield in different purifications. ACTC purified from bovine tissues generally yield at least 240 mgs with maximum concentrations of at least 5 mg/mL while ACTC purified insect cells yield around 3 mgs with maximum concentrations of 1.5 mg/mL. The maximum linear concentration range that Bradford Assay can pick up is generally 1.5 mg/mL (BioRad Instruction Manual). Thus, ACTC purified from WTrec was more accurate than ACTC purified from bovine cardiac using Bradford assay. With the disparity between WTrec and bovine ACTC, ACTC variants will be compared against WTrec ACTC due to the consistency of expression system and concentration determination method used.

4.7 Effect of E99K and R95C RTF in the actomyosin complex

I hypothesized that regulated actomyosin complexes including ACTC variants linked to HCM will exhibit a decrease in calcium sensitivity correlating to lower contractility in support of the global hypothesis of the HCM disease state. Based on my results, my hypothesis is supported. I observed that RTFs with HCM ACTC variants R95C and E99K have a lower pCa_{50} compared to WTrec, indicating less sensitivity to calcium.

Studies have shown that HCM is linked with an increase in calcium sensitivity (Kimura, 2010; Robinson et al., 2002; Watkins, 2001). Song *et al.* (2011) focused on the E99K ACTC and saw increased calcium sensitivity in mice and humans hearts compared to normal hearts using IVM. In contrast to my thesis, they worked with animal and human models that expressed E99K of less than 60%. Furthermore, they used higher ionic strength conditions for the IVM, which may introduce electrostatic shielding as described in **section 4.5**. Similar to my thesis, Debold *et al.* (2010) used the same buffer conditions for IVM, and expressed human ACTC in *Sf*9/baculovirus cell system and regulatory proteins from bovine hearts. They observed no shift in calcium sensitivity and only a reduced sliding speed. However, the filaments' velocities were found to be extremely low compared to literature (Gorga et al., 2003). The results from Song *et al.* (2011) and Debold *et al.* (2010) suggest that there might be differences between recombinant and tissue-purified ACTC proteins, and the experimental procedure that account for the increased pCa_{50} values that I observed.

To understand what is occurring in the protein-protein interactions, thin filament activation can be modeled by TM transitioning between three states based on availability

of calcium ions: blocked, closed, and open. To reiterate section **1.10**, in the blocked state, RTFs are unable to bind to myosin due to the absence of calcium ions and presence of TM blocking the myosin binding site. In the closed state, RTFs binding sites are partially revealed and can bind to myosin, but only weakly. Finally in the open state, myosin is able to bind strongly due to the saturation of calcium (Mckillop & Geeves, 1993). In RTFs, TM is positioned over subdomain 1 and 2 in the blocked state (Brown et al. 2005). Thus, the change from a glutamate negative residue to a lysine positive residue might promote electrostatic interactions with negatively charged TM, thereby favouring the closed state of RTFs (Brown et al., 2005; Cammarato et al., 2005; Debold et al., 2010; Mckillop & Geeves, 1993). This electrostatic interaction change may explain the decreased maximal motility between E99K and WTrec by preventing formation of cross-bridges between actin and myosin. It may also explain the decreased calcium sensitivity, as more calcium ions are needed to shift the Tn-TM complex to the open state.

Similar to E99K, R95C also resulted in decreased calcium sensitivity and sliding velocity, indicating that the RTF also favoured the closed state. One study that investigated R95C in the regulated form is by Noguchi *et al*. (2010). They found that RTFs with R95C exhibited a higher sensitivity to calcium compared to WT. They explained that the change from positively charged arginine to neutral charge cysteine may have decreased the binding to TM and shifted away from the blocked state. In contrast to my study with ACTC, they worked with skeletal actin expressed in yeast cells to investigate *Drosophila* muscles. This difference in actin species may be the reason why the decreased calcium sensitivity was observed, but it does not explain how the ACTC mutation substitution favoured the closed state.

4.8 Duty ratio of actomyosin with regulated ACTC variants

Surprisingly, the duty ratios of actomyosin with regulated ACTC variants were different compared to the duty ratios of actomyosin with unregulated ACTC variants. Despite the disparity between WTrec and bovine RTFs that was thoroughly discussed in **section 4.5**, the duty ratios were almost the same. These data suggest that although the calcium sensitivity was affected, the overall actomyosin interactions calculated from maximal activity and sliding speed of RTFs were not affected.

The duty ratio of actomyosin with regulated R95C ACTC yields the same duty ratio as WTrec RTFs, in comparison to the decreased duty ratio with unregulated R95C (**Figure 1**). This result suggests that the inclusion of Tn-TM complex compensated this defect. I speculate that the mechanism for this compensatory effect is similar to the mechanism in **section 4.1.1 and 4.6**. In unregulated R95C ACTC, the loss of electrostatic interaction potential would result in decreased binding of myosin to ACTC, causing decreased duty ratio that was observed. It was hypothesized by Homsher et al. (2003) that the presence of regulatory proteins causes a change in the actin sites that favours the binding of myosin. Hence, the effect of substitution mutation in regulated R95C ACTC was insignificant compared to the effect of Tn-TM on actomyosin interactions.

In contrast to R95C, regulated E99K resulted in different duty ratios. The change from increased duty ratio in unregulated form to a decreased duty ratio in regulated form can also be explained by the mechanism that was outlined in **section 4.6**. The electrostatic repulsion of myosin with unregulated E99K causes combination of decreased cross-bridge formation resulting in slower velocities in IVM assay and lower enzymatic activity resulted in an increased duty ratio. However, in the presence of

regulatory proteins, the positive residue of lysine binds to tropomyosin causing the RTFs to be in the closed state longer, and resulted in a decreased amount of time of regulated actomyosin interaction. The effect of substitution mutation in regulated E99K may be significant that it also affects the Tn-TM during contraction.

4.9 Summary of Discussion

Although my first hypothesis was not supported, the second hypothesis was supported with results clearly showing that there were molecular dysfunctions at the actomyosin complex with unregulated ACTC variants. The inclusion of Tn-TM complex compensated for the varying duty ratio of unregulated ACTC variants by altering the dynamics of actomyosin. Surprisingly, there was a decrease in calcium sensitivity which suggests a dysfunction between the interactions between ACTC and regulatory proteins. Importantly, Tn-Tm complex regulates the actomyosin and studies have shown that mutations in Tn and TM can affect the cross-bridge cycle and lead to either of disease phenotype (Mirza et al., 2005; Robinso et al., 2007; Watkins et al., 1995).

Chapter 5- Conclusion and Future Directions

5.1 Conclusions

CVDs affect both individuals and society. These diseases have been difficult to treat, especially HCM. Furthermore, current HCM medications target the diseases' symptoms and alleviate them temporarily, rather than treating the underlying problem. To develop more effective treatments, it is important to understand the molecular dysfunction of actomyosin interactions in HCM.

This thesis focuses on substitution mutations in subdomain 1 of ACTC (E99K, R95C, F90Δ, and H88Y) that are linked to HCM. The interaction between ACTC substitution mutations and myosin proteins can be experimentally observed through two assays: myosin ATPase, which measures enzymatic activity) and IVM which measures the motility of ACTC filaments and cross-bridge formation.

The first investigation was to observe unregulated thin filaments and its sole interaction with myosin. The ATPase data showed a decrease for all ACTC substitution mutation. However, in IVM, half of the ACTC substitution mutations (F90Δ and R95C) showed an increased velocity while the other half (E99K and H88Y) showed a decreased velocity when compared to WTrec. The values obtained from myosin ATPase and IVM was used to calculate the duty ratio, a marker for actomyosin interaction, and revealed different results: E99K exhibited increased duty ratio, F90Δ and R95C exhibited decreased duty ratios, and H88Y showed no change when compared to WTrec. These varying results did not support my first hypothesis and led me to consider that other factors may contribute to the actomyosin interaction, such as the regulation of thin filaments.

In the presence of Tn and TM, the actomyosin duty ratio for R95C was similar to WTrec indicating that the regulatory proteins compensated for the defect in electrostatic interaction. RTFs with E99K ACTC did not compensate for the increased duty ratio in unregulated form; instead, a decreased duty ratio was observed caused by electrostatic interactions between ACTC and TM and prolonging the inhibition of myosin binding. Independent to duty ratio, RTFs' handling of calcium was investigated using similar myosin ATPase and IVM assays. In regards to my second hypothesis, RTFs with R95C and E99K ACTC exhibit lower sensitivity to calcium. My results suggest that these ACTC substitution mutations might form interactions with the regulatory proteins and favour the "off state" thereby preventing myosin from binding. Overall, my results display the importance of Tn-TM and its role in the interaction between actin with substitution mutation in ACTC subdomain 1 and myosin.

The machinery of contraction in the heart is complex and involves many proteins and pathways, so it is very likely that combination of defects including the regulation of actomyosin would lead to HCM. The finding of R95C resulting in lower duty ratio in unregulated filament to obtaining duty ratio similar to WTrec in the presence of Tn-TM may further hypothesize that binding of myosin to actin may not be the primary dysfunction for some mutations resulting HCM, but perhaps an inefficiency in calcium handling and energetics. IVM and myosin ATPase confirmed that both R95C and E99K RTFs yield significantly higher pCa_{50} that WTrec. Furthermore, decreased absolute levels of phosphocreatine and ATP have been observed in HCM patients. In addition, there is a shift of energy substrate utilization from fatty acid oxidation to glucose utilization which results in a less efficient means of producing energy cardiomyocytes (Ashrafian et al.,

2003; Harvey & Leinwand, 2011; Ingwall, 2009; Jung et al., 2000). These finding may limit the actomyosin cycle and resulting in hypertrophy of cardiomyocytes (Ashrafian et al., 2003; Harvey & Leinwand, 2011; Ingwall, 2009; Jung et al., 2000).

5.2 Future Directions

Future improvements of these assays involve using cardiac myosin instead of skeletal muscle. Studies reveal that these myosins have different functionality and myosin ATPase activities (Andruchov et al., 2004; Katz et al., 1966). In addition, software to analyze motility of actin filaments would alleviate the burdens of analyzing single filaments by hand and prevent human biases. Currently, we have begun using FAST software to analyze all the filaments within a video.

In my experiments, one large assumption was the myosin step size, δ being 5 nm. Although Debold et al. (2010) noted no significant changes in rabbit cardiac myosin step size between WTrec and E99K, Uyeda et al. (1990) have noted the large discrepancy of myosin step size from factors such as density of HMM and the length of thin filaments. Furthermore, there are no studies on the myosin step size with other ACTC variants, which may have a profound impact on the duty ratio. Thus, the myosin step sizes of both unregulated and regulated form of ACTC variants must be investigated.

A TM fluorescent binding assay would confirm that the duty ratio was affected by the interaction of ACTC mutation substitution with TM as mentioned in the discussion section. Currently, there are no studies that investigated the binding properties of ACTC expressed from *Sf*21 insect cells with bovine cardiac Tn and TM. This experiment may help explain my results.

This thesis only analyzed RTFs with E99K and R95C ACTC. As mentioned in the investigation of unregulated thin filaments, there are two other substitution mutations on ACTC subdomain 1: F90Δ and H88Y. It would be interesting to see how their duty ratio and calcium sensitivity profile would respond in the regulated form. In addition, ACTC substitution mutations in subdomain 3 and 4 can be investigated due to the potential interaction with tropomyosin (Lorenz et al., 1995). Korman and Tobacman (1999) have already investigated yeast actin with double substitution mutations K315A/E316A and E311A/R312A and observed destabilization of RTFs and change in myosin ATPase activity.

Furthermore, the heart experiences continuous forces of load. In the assays performed, load was not introduced which fails to mimic the heart at physiological conditions. The addition of α-actinin would mimic the load within the sarcomere which myosin must overcome to move thin filaments. Jessica Wong, a project student that I supervised, found higher driving forces of myosin with unregulated H88Y, R95C, and F90Δ ACTC compared to WTrec, which suggest a longer binding time of actomyosin and increased ensemble force thereby leading to HCM (unpublished results). Continuing this study would investigate the higher driving forces of myosin with RTFs.

Although there are many more experiments and improvements to be done, these studies aim to determine the molecular dysfunction that is caused by HCM-linked mutations of ACTC, so that specific drugs that target the molecular dysfunction may alleviate the development of HCM. One drug in particular that is in development is *Omecamtiv Mecarbil*, which helps patients with symptoms of acute heart failure by targeting myosin and increase contraction (Teerlink et al., 2016).

References

Adelstein, R. S., & Tobacman, L. S. (1986). Mechanism of regulation of cardiac actin-myosin subfragment 1 by troponin-tropomyosin. *Biochemistry*, *25*(4), 798–802. https://doi.org/10.1021/bi00352a010

Aksel, T., ChoeYu, E., Sutton, S., Ruppel, K. M., & Spudich, J. A. (2015). Ensemble Force Changes that Result from Human Cardiac Myosin Mutations and a Small-Molecule Effector. *Cell Reports*, *11*(6), 910–920. https://doi.org/10.1016/j.celrep.2015.04.006

American Heart Association. (2014). What Is Cardiomyopathy in Adults?

American Heart Association. (2016). Hypertrophic Cardiomyopathy. Retrieved December 1, 2016, from http://www.heart.org/HEARTORG/Conditions/More/Cardiomyopathy/Hypertrophic-Cardiomyopathy_UCM_444317_Article.jsp#.WES2IuYrKUk

Andruchov, O., Wang, Y., Andruchova, O., & Galler, S. (2004). Functional properties of skinned rabbit skeletal and cardiac muscle preparations containing a-cardiac myosin heavy chain. *Pflugers Archiv European Journal of Physiology*, *448*(1), 44–53. https://doi.org/10.1007/s00424-003-1229-2

Anillo, M. (2015). *Hypertrophic cardiomyopathy-linked α-cardiac actin mutations and their role on actomyosin interactions*. University of Guelph.

Ashrafian, H., Redwood, C., Blair, E., & Watkins, H. (2003). Hypertrophic cardiomyopathy: A paradigm for myocardial energy depletion. *Trends in Genetics*. https://doi.org/10.1016/S0168-9525(03)00081-7

Behrmann, E. (2012). Structure of the Rigor Actin-Tropomyosin-Myosin Complex. *Cell*, *150*(2), 327–338.

Behrmann, E., Müller, M., Penczek, P. a., Mannherz, H. G., Manstein, D. J., & Raunser, S. (2012). Structure of the rigor actin-tropomyosin-myosin complex. *Cell*, *150*(1987), 327–338. https://doi.org/10.1016/j.cell.2012.05.037

Best, P. M., Donaldson, S. K., & Kerrick, W. G. (1977). Tension in mechanically disrupted mammalian cardiac cells: effects of magnesium adenosine triphosphate. *J Physiol*, *265*(1), 1–17.

Billeter, R., Weber, H., Lutz, H., Howald, H., Eppenberger, H. M., & Jenny, E. (1980). Myosin types in human skeletal muscle fibers. *Histochemistry*, *65*(3), 249–259. https://doi.org/10.1007/BF00493174

Bloom, D. E., Cafiero, E., Jané-Llopis, E., Abrahams-Gessel, S., Reddy Bloom, L., Fathima, S., … Weiss, J. (2011). The Global Economic Burden of Noncommunicable Diseases. *World Economic Forum*, (September), 1–46. Retrieved from http://ideas.repec.org/p/gdm/wpaper/8712.html

Bookwalter, C. S., & Trybus, K. M. (2006). Functional consequences of a mutation in an expressed human alpha-cardiac actin at a site implicated in familial hypertrophic cardiomyopathy. *The Journal of Biological Chemistry*, *281*(24), 16777–84. https://doi.org/10.1074/jbc.M512935200

Bradford, M. M. (1976). A rapid and sensitive method for the quantitation of protein utilizing the principle of protein-dye binding. *Anal. Biochem.*, *72*, 248–254. https://doi.org/10.1016/0003-2697(76)90527-3

Brown, J. H., Zhou, Z., Reshetnikova, L., Robinson, H., Yammani, R. D., Tobacman, L.

S., & Cohen, C. (2005). Structure of the mid-region of tropomyosin: bending and binding sites for actin. *Proceedings of the National Academy of Sciences of the United States of America*, *102*(52), 18878–18883. https://doi.org/10.1073/pnas.0509269102

Buzan, J., Du, J., Karpova, T., & Frieden, C. (1999). Histidine-tagged wild-type yeast actin: its properties and use in an approach for obtaining yeast actin mutants. *Proceedings of the National Academy of Sciences of the United States of America*, *96*, 2823–2827. https://doi.org/10.1073/pnas.96.6.2823

Cammarato, A., Craig, R., Sparrow, J. C., & Lehman, W. (2005). E93K charge reversal on actin perturbs steric regulation of thin filaments. *Journal of Molecular Biology*, *347*(5), 889–894. https://doi.org/10.1016/j.jmb.2005.02.022

Carniel, E., Taylor, M. R. G., Sinagra, G., Di Lenarda, A., Ku, L., Fain, P. R., … Mestroni, L. (2005). Alpha-myosin heavy chain: a sarcomeric gene associated with dilated and hypertrophic phenotypes of cardiomyopathy. *Circulation*, *112*(1), 54–9. https://doi.org/10.1161/CIRCULATIONAHA.104.507699

Chung, M.-W., Tsoutsman, T., & Semsarian, C. (2003). Hypertrophic cardiomyopathy: from gene defect to clinical disease. *Cell Research*, *13*(1), 9–20. https://doi.org/10.1038/sj.cr.7290146

Clemmens, E. W., & Regnier, M. (2004). Skeletal regulatory proteins enhance thin filament sliding speed and force by skeletal HMM. *Journal of Muscle Research and Cell Motility*, *25*(7), 515–525. https://doi.org/10.1007/s10974-004-3787-0

Cooper, G. M., & Hausman, R. E. (2007). *The Cell: A Molecular Approach*. *Sinauer Associates*.

D.C. Hellam, R. J. P., Hellam, D., & Podolsky, R. (1969). Force measurements in skinned muscle fibres. *Journal of Physiology*, *200*, 807–819. https://doi.org/10.1113/jphysiol.1969.sp008723

Dahari, M., & Dawson, J. F. (2015). Do cardiac actin mutations lead to altered actomyosin interactions? *Biochemistry and Cell Biology = Biochimie et Biologie Cellulaire*, *93*(4), 330–4. https://doi.org/10.1139/bcb-2014-0156

Daughenbaugh, L. A. (2007). Cardiomyopathy : An Overview, (April).

De La Cruz, E. M., Wells, A. L., Rosenfeld, S. S., Ostap, E. M., & Sweeney, H. L. (1999). The kinetic mechanism of myosin V. *Proc Natl Acad Sci*, *96*(24), 13726–13731. https://doi.org/10.1073/pnas.96.24.13726

Debold, E. P., Saber, W., Cheema, Y., Bookwalter, C. S., Trybus, K. M., Warshaw, D. M., & VanBuren, P. (2010). Human actin mutations associated with hypertrophic and dilated cardiomyopathies demonstrate distinct thin filament regulatory properties in vitro. *Journal of Molecular and Cellular Cardiology*, *48*, 286–292. https://doi.org/10.1016/j.yjmcc.2009.09.014

Donaldson, S. K., & Kerrick, W. G. (1975). Characterization of the effects of Mg2+ on Ca2+- and Sr2+-activated tension generation of skinned skeletal muscle fibers. *J Gen Physiol.*, *66*(4), 427–444.

Ebashi, S., & Endo, M. (1968). Calcium ion and muscle contraction. *Prog. Biophys. Mol. Biol.*, *18*(123).

Eyk, J. E. Van, Thomas, L. T., Tripet, B., Wiesner, R. J., Pearlstone, J. R., Farah, C. S., … Hodges, R. S. (1997). Distinct Regions of Troponin I Regulate Ca2+-dependent Activation and Ca2+ Sensitivity of the Acto-S1-TM ATPase Activity of the Thin

Filament. *Journal of Biological Chemistry*, *272*(16), 10529–10537.
Fabiato, A., & Fabiato, F. (1975). Effects of magnesium on contractile activation of skinned cardiac cells. *J Physiol*, *249*(3), 497–517.
Farah, C. S., & Reinach, F. C. (1995). The troponin complex and regulation of muscle contraction. *The FASEB Journal*, *9*, 755–767. https://doi.org/10.1096/fj.02-0402fje
Fraser, I. D. C., & Marston, S. B. (1995). In vitro motility analysis of actin-tropomyosin regulation by troponin and calcium. The thin filament is switched as a single cooperative unit. *Journal of Biological Chemistry*. https://doi.org/10.1074/jbc.270.14.7836
Gafurov, B., & Chalovich, J. M. (2007). Equilibrium distribution of skeletal actin-tropomyosin-troponin states, determined by pyrene-tropomyosin fluorescence. *FEBS Journal*, *274*(9), 2287–2299. https://doi.org/10.1111/j.1742-4658.2007.05765.x
Gehlert, S., Bloch, W., & Suhr, F. (2015). Ca2+-Dependent Regulations and Signaling in Skeletal Muscle: From Electro-Mechanical Coupling to Adaptation. *International Journal of Molecular Sciences*, *16*(1), 1066–1095. https://doi.org/10.3390/ijms16011066
Gomes, A. V, Potter, J. D., & Szczesna-cordary, D. (2002). The Role of Troponins in Muscle Contraction. *IUBMB Life*, 323–333. https://doi.org/10.1080/15216540290114676
Goody, R. S. (2003). The missing link in the muscle cross-bridge cycle. *Nature Structural Biology*, *10*, 773–775. https://doi.org/10.1038/nsb1003-773
Gordon, A. M., Godt, R. E., Donaldson, S. K., & Harris, C. E. (1973). Tension in skinned frog muscle fibers in solutions of varying ionic strength and neutral salt composition. *The Journal of General Physiology*, *62*(5), 550–574. https://doi.org/10.1085/jgp.62.5.550
Gordon, A. M., Homsher, E., & Regnier, M. (2000). Regulation of contraction in striated muscle. *Physiological Reviews*, *80*, 853–924.
Gordon, a M., LaMadrid, M. a, Chen, Y., Luo, Z., & Chase, P. B. (1997). Calcium regulation of skeletal muscle thin filament motility in vitro. *Biophysical Journal*, *72*(3), 1295–1307. https://doi.org/10.1016/S0006-3495(97)78776-9
Gorga, J. a, Fishbaugher, D. E., & VanBuren, P. (2003). Activation of the Calcium-Regulated Thin Filament by Myosin Strong Binding. *Biophysical Journal*, *85*(4), 2484–2491. https://doi.org/10.1016/S0006-3495(03)74671-2
Greaser, M. L., & Gergely, J. (1973). Purification and Properties of the Components from Troponin and Properties of the Components from Troponin. *The Journal of Biological Chemistry*, *248*(6), 2125–2133.
Greaser, M. L., & Gergely, J. J. (1971). Three Protein Components Reconstitution of Troponin Protein Components. *J. Biol. Chem.*, *246*, 4226–4233.
Gulati,Jagdish; Podolsky, J. R. (1978). Contraction Transients of Skinned Muscle Fibers " Effects of Calcium and Ionic Strength. *Journal of General Physiology*, *72*(November), 701–715.
Harris, D. E., & Warshaw, D. M. (1993). Smooth and skeletal muscle myosin both exhibit low duty cycles at zero load in vitro. *Journal of Biological Chemistry*, *268*(20), 14764–14768.
Harvey, P. A., & Leinwand, L. A. (2011). Cellular mechanisms of cardiomyopathy. *Journal of Cell Biology*. https://doi.org/10.1083/jcb.201101100

Hill, A. V. (1910). The possible effects of the aggregation of the molecules of hæmglobin on it's dissociation curves. *Journal of Physiology*, *40*. https://doi.org/10.1113/jphysiol.1910.sp001386

Homsher, E., Kim, B., Bobkova, a, & Tobacman, L. S. (1996). Calcium regulation of thin filament movement in an in vitro motility assay. *Biophysical Journal*, *70*(April), 1881–1892. https://doi.org/10.1016/S0006-3495(96)79753-9

Homsher, E., Lee, D. M., Morris, C., Pavlov, D., & Tobacman, L. S. (2000). Regulation of force and unloaded sliding speed in single thin filaments: effects of regulatory proteins and calcium. *The Journal of Physiology*, *524 Pt 1*, 233–243. https://doi.org/10.1111/j.1469-7793.2000.00233.x

Homsher, E., Nili, M., Chen, I. Y., & Tobacman, L. S. (2003). Regulatory Proteins Alter Nucleotide Binding to Acto-Myosin of Sliding Filaments in Motility Assays. *Biophysical Journal*, *85*(2), 1046–1052. https://doi.org/10.1016/S0006-3495(03)74543-3

Homsher, E., Wang, F., & Sellers, J. R. (1992). Factors affecting movement of F-actin filaments propelled by skeletal muscle heavy meromyosin. *American Journal of Physiology - Cell Physiology*, *262*(3), C714–C723. Retrieved from http://www.ncbi.nlm.nih.gov/pubmed/1550212%5Cnhttp://ajpcell.physiology.org/content/262/3/C714.full-text.pdf+html

Huxley, H. E. (1973). Structural changes in the actin- and myosin-containing filaments [of muscle] during contraction. *Cold Spring Harbor Symposia on Quantitative Biology*, *37*, 361–376. https://doi.org/10.1101/SQB.1973.037.01.046

Ingwall, J. S. (2009). Energy metabolism in heart failure and remodelling. *Cardiovascular Research*, *81*(3), 412–419. https://doi.org/10.1093/cvr/cvn301

Jarcho, J. A., McKenna, W., Pare, J. A., Solomon, S. D., Holcombe, R. F., Dickie, S., … Seidman, C. E. (1989). Mapping a gene for familial hypertrophic cardiomyopathy to chromosome 14q1. *The New England Journal of Medicine*, *321*, 1372–1378. https://doi.org/10.1056/NEJM198911163212005

Jung, W. I., Hoess, T., Bunse, M., Widmaier, S., Sieverding, L., Breuer, J., … Lutz, O. (2000). Differences in cardiac energetics between patients with familial and nonfamilial hypertrophic cardiomyopathy. *Circulation*, *101*(12), E121–E121. https://doi.org/10.1161/01.CIR.101.12.e121

Karibe, A., Tobacman, L. S., Strand, J., Butters, C., Back, N., Bachinski, L. L., … Fananapazir, L. (2001). Hypertrophic Cardiomyopathy Caused by a Novel a-Tropomyosin Mutation (V95A) Is Associated With Mild Cardiac Phenotype, Abnormal Calcium Binding to Troponin, Abnormal Myosin Cycling, and Poor Prognosis. *Circulation*, *103*, 65–71. https://doi.org/10.1161/01.CIR.103.1.65

Kaski, J. P., Syrris, P., Esteban, M. T. T., Jenkins, S., Pantazis, A., Deanfield, J. E., … Elliott, P. M. (2009). Prevalence of Sarcomere Protein Gene Mutations in Preadolescent Children With Hypertrophic CardiomyopathyCLINICAL PERSPECTIVE. *Circulation: Cardiovascular Genetics*, *2*(5), 436–441. https://doi.org/10.1161/CIRCGENETICS.108.821314

Katz, A. M., Repke, D. I., & Rubin, B. B. (1966). Adenosinetriphosphatase Activity of Cardiac Myosin: Comparison of the Enzymatic Activities and Activation by Actin of Dog Cardiac, Rabbit Cardiac, Rabbit White Skeletal and Rabbit Red Skeletal Muscle Myosins. *Circulation Research*, *19*(3), 611–621.

https://doi.org/10.1161/01.res.19.3.611
Katz, a M. (1967). Regulation of cardiac muscle contractility. *The Journal of General Physiology*, *50*(6), Suppl:185-96. https://doi.org/10.1085/jgp.50.6.185
Kimura, A. (2010). Molecular basis of hereditary cardiomyopathy: abnormalities in calcium sensitivity, stretch response, stress response and beyond. *Journal of Human Genetics*, *55*(2), 81–90. https://doi.org/10.1038/jhg.2009.138
Kolappan, S., Gooch, J. T., Weeds, A. G., & McLaughlin, P. J. (2003). Gelsolin domains 4-6 in active, actin-free conformation identifies sites of regulatory calcium ions. *Journal of Molecular Biology*, *329*(1), 85–92. https://doi.org/10.1016/S0022-2836(03)00383-8
Korman, V. L., & Tobacman, L. S. (1999). Mutations in Actin Subdomain 3 That Impair Thin Filament Regulation by Troponin and Tropomyosin. *The Journal of Biological Chemistry*, *274*(32), 22191–22196.
Kumar, A., Crawford, K., Close, L., Madison, M., Lorenz, J., Doetschman, T., … Lessard, J. L. (1997). Rescue of cardiac alpha-actin-deficient mice by enteric smooth muscle gamma-actin. *Proceedings of the National Academy of Sciences of the United States of America*, *94*(9), 4406–4411.
Laemmli, U. K. (1970): (1970). Cleavage of Structural Proteins during Assembly of Head of Bacteriophage-T4. *Nature*, *227*. https://doi.org/10.1038/227680a0
Lakdawala, N. K., Funke, B. H., Baxter, S., Cirino, A. L., Roberts, A. E., Judge, D. P., … Ho, C. Y. (2012). Genetic testing for dilated cardiomyopathy in clinical practice. *Journal of Cardiac Failure*, *18*(4), 296–303. https://doi.org/10.1016/j.cardfail.2012.01.013
Lin, D., Bobkova, a, Homsher, E., & Tobacman, L. S. (1996). Altered cardiac troponin T in vitro function in the presence of a mutation implicated in familial hypertrophic cardiomyopathy. *The Journal of Clinical Investigation*, *97*(12), 2842–8. https://doi.org/10.1172/JCI118740
Lorenz, M., & Holmes, K. C. (2010). The actin-myosin interface. *Proceedings of the National Academy of Sciences*, *107*(28), 12529–12534. https://doi.org/10.1073/pnas.1003604107
Lorenz, M., Poole, K. J., Popp, D., Rosenbaum, G., & Holmes, K. C. (1995). An atomic model of the unregulated thin filament obtained by X-ray fiber diffraction on oriented actin-tropomyosin gels. *Journal of Molecular Biology*, *246*(April), 108–119. https://doi.org/10.1006/jmbi.1994.0070
MacIntosh, B. R. (2003). Role of calcium sensitivity modulation in skeletal muscle performance. *News Physiol Sci*, *18*, 222–225. https://doi.org/10.1152/nips.01456.2003
Mackrill, J. J. (1999). Protein – protein interactions in intracellular Ca2+ -release channel function. *Journal of Biochemistry*, *361*, 345–361.
Margossian, S.S.; Lowey, S. (1982). Preparation of myosin and its subfragments from rabbit skeletal muscle. *Meth Enzymol*, *85 Pt B*, 55–71.
Marian, A., & Roberts, R. (2001). The molecular genetic basis for hypertrophic cardiomyopathy. *Journal of Molecular and Cellular Cardiology*, *33*(4), 655–70. https://doi.org/10.1006/jmcc.2001.1340.The
Marks, A. R. (2013). Calcium cycling proteins and heart failure: mechanisms and therapeutics. *The Journal of Clinical Investigation*, *123*(1).

https://doi.org/10.1172/JCI62834.46
Mather, J.P., and P. E. R. (1998). *Introduction to Cell and Tissue Culture: Theory and Technique*. *Plenum Press*. New York and London.
Mckillop, D. F. A., & Geeves, M. A. (1993). Regulation of the Interaction between Actin and Myosin Subfragment 1: Evidence for Three States of the Thin Filament. *Biophysical Journal Volume, 65*, 693–701. https://doi.org/10.1016/S0006-3495(93)81110-X
Mirza, M., Marston, S., Willott, R., Ashley, C., Mogensen, J., McKenna, W., … Watkins, H. (2005). Dilated cardiomyopathy mutations in three thin filament regulatory proteins result in a common functional phenotype. *Journal of Biological Chemistry*, *280*(31), 28498–28506. https://doi.org/10.1074/jbc.M412281200
Mogensen, J., Klausen, I. C., Pedersen, a K., Egeblad, H., Bross, P., Kruse, T. a, … Borglum, a D. (1999). Alpha-cardiac actin is a novel disease gene in familial hypertrophic cardiomyopathy. *The Journal of Clinical Investigation*, *103*(10), R39-43. https://doi.org/10.1172/JCI6460
Mogensen, J., Perrot, A., Andersen, P., Havndrup, O., Klausen, I., Christiansen, M., … Borglum, A. (2004). Clinical and genetic characteristics of α cardiac actin gene mutations in hypertrophic cardiomyopathy. *Journal of Medical Genetics*, *41*(1), e10. https://doi.org/10.1136/jmg.2003.010447
Molloy, J. E., Burns, J. E., Kendrick-Jones, J., Tregear, R. T., & White, D. C. S. (1995). Movement and force produced by a single myosin head. *Nature*, *378*(6553), 209–212. https://doi.org/10.1038/378209a0
Moore, J. R., Leinwand, L., & Warshaw, D. M. (2012). Understanding cardiomyopathy phenotypes based on the functional impact of mutations in the myosin motor. *Circulation Research*, *111*(3), 375–85. https://doi.org/10.1161/CIRCRESAHA.110.223842
Morimoto, S. (2008). Sarcomeric proteins and inherited cardiomyopathies. *Cardiovascular Research*, *77*(4), 659–66. https://doi.org/10.1093/cvr/cvm084
Morita, H., Rehm, H. L., Menesses, A., McDonough, B., Roberts, A. E., Kucherlapati, R., … Seidman, C. E. (2008). Shared genetic causes of cardiac hypertrophy in children and adults. *The New England Journal of Medicine*, *358*(18), 1899–1908. https://doi.org/10.1056/NEJMoa075463
Mundia, M. M., Demers, R. W., Chow, M. L., Perieteanu, A. a, & Dawson, J. F. (2012). Subdomain location of mutations in cardiac actin correlate with type of functional change. *PloS One*, *7*(5), e36821. https://doi.org/10.1371/journal.pone.0036821
Narolska, N. A., van Loon, R. B., Boontje, N. M., Zaremba, R., Penas, S. E., Russell, J., … Stienen, G. J. M. (2005). Myocardial contraction is 5-fold more economical in ventricular than in atrial human tissue. *Cardiovascular Research*, *65*(1), 221–229. https://doi.org/10.1016/j.cardiores.2004.09.029
Noguchi, T. Q. P., Gomibuchi, Y., Murakami, K., Ueno, H., Hirose, K., Wakabayashi, T., & Uyeda, T. Q. P. (2010). Dominant negative mutant actins identified in flightless Drosophila can be classified into three classes. *Journal of Biological Chemistry*, *285*(7), 4337–4347. https://doi.org/10.1074/jbc.M109.059881
O'Reilly, D. R., Miller, L. K., & Luckow, V. A. (1994). Baculovirus Expression Vectors: A Laboratory Manual. *Oxford University Press, New York U.a.* Retrieved from http://books.google.com/books?hl=de&lr=&id=lP8VFRX8zHMC&pgis=1

Ohki, T., Ohno, C., Oyama, K., Mikhailenko, S. V., & Ishiwata, S. (2009). Purification of cytoplasmic actin by affinity chromatography using the C-terminal half of gelsolin. *Biochemical and Biophysical Research Communications*, *383*(1), 146–150. https://doi.org/10.1016/j.bbrc.2009.03.144

Olivotto, I., Girolami, F., Ackerman, M. J., Nistri, S., Bos, J. M., Zachara, E., … Cecchi, F. (2008). Myofilament protein gene mutation screening and outcome of patients with hypertrophic cardiomyopathy. *Mayo Clinic Proceedings*, *83*(6), 630–638. https://doi.org/10.4065/83.6.630

Olson, T. M., Doan, T. P., Kishimoto, N. Y., Whitby, F. G., Ackerman, M. J., & Fananapazir, L. (2000). Inherited and de novo mutations in the cardiac actin gene cause hypertrophic cardiomyopathy. *Journal of Molecular and Cellular Cardiology*, *32*(9), 1687–94. https://doi.org/10.1006/jmcc.2000.1204

Olson, T. M., Michels, V. V., Thibodeau, S. N., Tai, Y. S., & Keating, M. T. (1998). Actin mutations in dilated cardiomyopathy, a heritable form of heart failure. *Science (New York, N.Y.)*, *280*(5364), 750–752.

Ottolia, M., Torres, N., Bridge, J. H. B., Philipson, K. D., & Goldhaber, J. I. (2013). Na/Ca exchange and contraction of the heart. *Journal of Molecular and Cellular Cardiology*, *61*, 28–33. https://doi.org/10.1016/j.yjmcc.2013.06.001

Parry, D A D; Squire, J. M. (1973). Structural Role of Tropomyosin in Muscle Regulation : Analysis of the X-ray Diffraction Patterns from Relaxed and Contracting Muscles, 33–55.

Patel, V., Critoph, C. H., Finlay, M. C., Mist, B., Lambiase, P. D., & Elliott, P. M. (2014). Heart rate recovery in patients with hypertrophic cardiomyopathy. *The American Journal of Cardiology*, *113*(6), 1011–7. https://doi.org/10.1016/j.amjcard.2013.11.062

Perrin, B. J., & Ervasti, J. M. (2010). The actin gene family: Function follows isoform. *Cytoskeleton*, *67*(August), 630–634. https://doi.org/10.1002/cm.20475

Redwood, C. S., Moolman-Smook, J. C., & Watkins, H. (1999). Properties of mutant contractile proteins that cause hypertrophic cardiomyopathy. *Cardiovascular Research*, *44*(1), 20–36. https://doi.org/10.1016/S0008-6363(99)00213-8

Reiser, P. J., Moss, R. L., Giulian, G. G., & Greaser, M. L. (1985). Shortening velocity in single fibers from adult rabbit soleus muscles is correlated with myosin heavy chain composition. *Journal of Biological Chemistry*, *260*(16), 9077–9080.

Reiser, P. J., Portman, M. A., Ning, X. H., & Schomisch Moravec, C. (2001). Human cardiac myosin heavy chain isoforms in fetal and failing adult atria and ventricles. *American Journal of Physiology. Heart and Circulatory Physiology*, *280*(4), H1814-1820.

Robinson, P., Griffiths, P. J., Watkins, H., & Redwood, C. S. (2007). Dilated and hypertrophic cardiomyopathy mutations in troponin and ??-tropomyosin have opposing effects on the calcium affinity of cardiac thin filaments. *Circulation Research*, *101*(12), 1266–1273. https://doi.org/10.1161/CIRCRESAHA.107.156380

Robinson, P., Mirza, M., Knott, A., Abdulrazzak, H., Willott, R., Marston, S., & Hugh Watkins, C. R. (2002). Alterations in thin filament regulation induced by a human cardiac troponin T mutant that causes dilated cardiomyopathy are distinct from those induced by troponin T mutants that cause hypertrophic cardiomyopathy. *Journal of Biological Chemistry*, *277*(43), 40710–40716.

https://doi.org/10.1074/jbc.M203446200
Rüegg, C., Veigel, C., Molloy, J. E., Schmitz, S., Sparrow, J. C., & Fink, R. H. A. (2002). Molecular motors: force and movement generated by single myosin II molecules. *American Physiological Society*, *17*, 213–8. https://doi.org/10.1152/nips.01389.2002
Rutkevich, L. a, Teal, D. J., & Dawson, J. F. (2006). Expression of actin mutants to study their roles in cardiomyopathy. *Canadian Journal of Physiology and Pharmacology*, *84*(1), 111–9. https://doi.org/10.1139/Y05-140
Scellini, B., Piroddi, N., Flint, G. V, Regnier, M., Poggesi, C., & Tesi, C. (2014). Impact of tropomyosin isoform composition on fast skeletal muscle thin filament regulation and force development. *J Muscle Res Cell Motil*, *1*. https://doi.org/10.1007/s10974-014-9394-9
Seidman, J. G., & Seidman, C. (2001). The Genetic Basis for Cardiomyopathy. *Cell*, *104*(4), 557–567. https://doi.org/10.1016/S0092-8674(01)00242-2
Shchepkin, D. V., Kopylova, G. V., & Nikitina, L. V. (2011). Study of reciprocal effects of cardiac myosin and tropomyosin isoforms on actin-myosin interaction with in vitro motility assay. *Biochemical and Biophysical Research Communications*, *415*(1), 104–108. https://doi.org/10.1016/j.bbrc.2011.10.022
Sommese, R. F., Sung, J., Nag, S., Sutton, S., Deacon, J. C., Choe, E., … Spudich, J. A. (2013). Molecular consequences of the R453C hypertrophic cardiomyopathy mutation on human β-cardiac myosin motor function. *Proceedings of the National Academy of Sciences*, *110*(31), 12607–12612. https://doi.org/10.1073/pnas.1309493110
Song, W., Dyer, E., Stuckey, D. J., Copeland, O., Leung, M.-C., Bayliss, C., … Marston, S. B. (2011). Molecular mechanism of the E99K mutation in cardiac actin (ACTC Gene) that causes apical hypertrophy in man and mouse. *The Journal of Biological Chemistry*, *286*(31), 27582–93. https://doi.org/10.1074/jbc.M111.252320
Spudich, J. A., & Watt, S. (1971). The regulation of rabbit skeletal muscle contraction. *Journal of Biological Chemistry*, *246*(15), 4866.
Sun, H. Q., Yamamoto, M., Mejillano, M., & Yin, H. L. (1999). Gelsolin, a Multifunctional Actin Regulatory Protein. *The Journal of Biological Chemistry*, *274*(32), 33179–33182.
Swartz, D. R., & Moss, R. L. (2001). Strong binding of myosin increases shortening velocity of rabbit skinned skeletal muscle fibres at low levels of Ca2+. *Journal of Physiology*, *533*(2), 357–365. https://doi.org/10.1111/j.1469-7793.2001.0357a.x
Sweeney, H. L., Feng, H. S., Yang, Z., Watkins, H., & Pollard, T. D. (1998). Functional analyses of troponin T mutations that cause hypertrophic cardiomyopathy: Insights into disease pathogenesis and troponin function. *Medical Sciences*, *95*(November), 14406–14410. https://doi.org/10.1073/pnas.95.24.14406
Teerlink, J. R., Felker, G. M., McMurray, J. J. V, Ponikowski, P., Metra, M., Filippatos, G. S., … Wasserman, S. M. (2016). Acute Treatment with Omecamtiv Mecarbil to Increase Contractility in Acute Heart Failure: The ATOMIC-AHF Study. *Journal of the American College of Cardiology*, *67*(12), 1444–1455. https://doi.org/10.1016/j.jacc.2016.01.031
Terman, J. R., & Kashina, A. (2014). Post-translational modification and Regulation of Actin. *Current Opinion in Cell Biology*, *25*(1), 30–38. https://doi.org/10.1016/j.ceb.2012.10.009.Post-translational

Trybus, K. M. (2000). Biochemical studies of myosin. *Methods (San Diego, Calif.)*, *22*(4), 327–35. https://doi.org/10.1006/meth.2000.1085

Uyeda, T. Q. P., Kron, S. J., & Spudich, J. A. (1990). Myosin step size. Estimation from slow sliding movement of actin over low densities of heavy meromyosin. *Journal of Molecular Biology*, *214*(3), 699–710. https://doi.org/10.1016/0022-2836(90)90287-V

Van Driest, S. L., Ellsworth, E. G., Ommen, S. R., Tajik, a J., Gersh, B. J., & Ackerman, M. J. (2003). Prevalence and spectrum of thin filament mutations in an outpatient referral population with hypertrophic cardiomyopathy. *Circulation*, *108*(4), 445–51. https://doi.org/10.1161/01.CIR.0000080896.52003.DF

VanBuren, P., Alix, S. L., Gorga, J. a, Begin, K. J., LeWinter, M. M., & Alpert, N. R. (2002). Cardiac troponin T isoforms demonstrate similar effects on mechanical performance in a regulated contractile system. *American Journal of Physiology. Heart and Circulatory Physiology*, *282*(5), H1665-71. https://doi.org/10.1152/ajpheart.00938.2001

Vandekerckhove, J., Bugaisky, G., & Buckingham, M. (1986). Simultaneous expression of skeletal muscle and heart actin proteins in various striated muscle tissues and cells. A quantitative determination of the two actin isoforms. *Journal of Biological Chemistry*, *261*(4), 1838–1843.

Velden, J. Van Der, Papp, Z., Zaremba, R., Boontje, N. M., Jong, J. W. De, & Owen, V. J. (2003). I ncreased Ca 2 1 -sensitivity of the contractile apparatus in end-stage human heart failure results from altered phosphorylation of contractile proteins. *Cardiovascular Research*, *57*, 37–47.

Vinogradova, M. V, Stone, D. B., Malanina, G. G., Karatzaferi, C., Cooke, R., Mendelson, R. A., & Fletterick, R. J. (2005). Ca(2+)-regulated structural changes in troponin. *Proceedings of the National Academy of Sciences of the United States of America*, *102*(14), 5038–43. https://doi.org/10.1073/pnas.0408882102

Walker, J. S., Li, X., & Buttrick, P. M. (2010). Analysing force–pCa curves. *J Muscle Res Cell Motil*, *31*(1), 59–69. https://doi.org/10.1007/s10974-010-9208-7.Analysing

Watkins, H. (2001). Hypertrophic cardiomyopathy : from molecular and genetic mechanisms to clinical management. *European Heart Journal*, *3*, 43–50.

Watkins, H., McKenna, W. J., Thierfelder, L., Suk, H. J., Anan, R., O'Donoghue, A., … Seidman, J. G. (1995). Mutations in the genes for cardiac troponin T and alpha-tropomyosin in hypertrophic cardiomyopathy. *The New England Journal of Medicine*, *332*(16), 1058–64. https://doi.org/10.1056/NEJM199504203321603

Weber, A., & Murray, J. M. (1973). Molecular control mechanisms in muscle contraction. *Physiological Reviews*, *53*(3), 612–673.

Wigle, E. D., Sasson, Z., Henderson, M. A., Ruddy, T. D., Fulop, J., Rakowski, H., & Williams, W. G. (1985). Hypertrophic cardiomyopathy. The importance of the site and the extent of hypertrophy. A review. *Progress in Cardiovascular Diseases*. https://doi.org/10.1016/0033-0620(85)90024-6

World Health Organization. (2011). *Global status report on noncommunicable diseases 2010*. Geneva. Retrieved from http://apps.who.int/iris/bitstream/10665/44579/1/9789240686458_eng.pdf

World Health Organization. (2016). Cardiovascular diseases (CVDs). Retrieved December 1, 2016, from http://www.who.int/mediacentre/factsheets/fs317/en/

Yoko Yano Toyoshima ; Stephen J. Kron ; Elizabeth M. Mcnally ; Kenneth R. Niebling ; Chikashi Toyoshima ; James A. Spudich. (1987). Myosin subfragment-1 is sufficient to move actin filaments in vitro. *Nature*.

Zarain-Herzberg, A., Estrada-Avilés, R., & Fragoso-Medina, J. (2012). Regulation of sarco(endo)plasmic reticulum Ca2+-ATPase and calsequestrin gene expression in the heart. *Canadian Journal of Physiology and Pharmacology*, *90*(8), 1017–28. https://doi.org/10.1139/y2012-057

Zot, A. S., & Potter, J. D. (1987). Structural aspects of troponin-tropomyosin regulation of skeletal muscle contraction. *Annual Review of Biophysics*, *16*, 535–59.